Logistics Planning for Direct Temporary Disaster Housing Assistance under Demand Uncertainty

Sheng-Yin Chen[a], Yongjia Song[a,*], Dustin Albright[b] and Weichiang Pang[c]

[a]Department of Industrial Engineering, Clemson University, Clemson, 29634, SC, United States
[b]School of Architecture, Clemson University, Clemson, 29634, SC, United States
[c]Department of Civil Engineering, Clemson University, Clemson, 29634, SC, United States

ARTICLE INFO

Keywords:
Disaster Housing Recovery
Logistics Planning
Optimization under Uncertainty
Spatial Regression Model

ABSTRACT

In this paper, we propose and study a framework for disaster housing logistics planning under demand uncertainty. Specifically, we utilize a two-stage chance-constrained stochastic programming model to achieve the balance between logistics operational cost and demand fulfillment especially towards extreme disaster scenarios. To do so, we incorporate two operational modalities, one for the ordinary modality and the other for the emergency modality, and the emergency modality is only allowed to be activated for a certain percentage of scenarios that is specified by the decision maker among all scenarios. The set of scenarios is generated according to a spatial regression model for characterizing the disaster housing demand based on a selected number of independent variables related to both the hazard and socioeconomic factors, which is trained offline from historical data. We conduct a numerical experiment based on Hurricane Ian, and our numerical results show the effectiveness of the proposed approach compared to some standard benchmark approaches. We also highlight the managerial insights for disaster housing logistics planning gained through this numerical experiment.

1. Introduction

Direct housing is one of the most critical resources following disaster displacement. When confronted with large-scale foreseeable disasters like flooding and hurricanes, individuals are displaced from their homes or habitual dwellings to avoid the impacts. In the United States (US), the frequency and severity of displacements linked to disasters have seen a consistent rise in recent decades (Deng, 2001). Although disaster displacement endeavors to minimize human exposure to natural hazards and reduce the risk of direct injuries resulting from disasters, prolonged displacement caused by a disaster event has been shown to result in significant social issues, such as unemployment and mental illness (Hori and Schafer, 2010). In order to mitigate the social costs caused by these issues, direct housing emerges as one of the critical resources employed to alleviate the suffering of displaced victims in the current practice of the Federal Emergency Management Agency (FEMA) of US. Its significance is further accentuated in extreme circumstances, as direct housing is regarded as the "last resort" (FEMA, 2020) in the entire spectrum of disaster housing assistance, after alternative housing resources such as the rental units are exhausted.

One of the challenges in disaster housing logistics planning is to effectively address the disaster housing demand uncertainty (Katrina, 2007; Laura Layden, 2022; National Low Income Housing Coalition, 2018). For instance, during Hurricane Harvey, approximately 30,000 families endured prolonged displacement in emergency shelters for at least one month (Pam Fessler, 2017). Similarly, in the aftermath of Hurricane Sandy, around 11,000 families found themselves in shelters for nearly six weeks following the storm (Patrick Adcroft, 2022). The absence of a comprehensive logistics plan for direct housing assistance can result in extended periods of displacement during major disasters, exceeding initial expectations. This motivates us to develop a framework for direct housing logistics planning, offering an efficient logistical plan that leads to a timely fulfillment of disaster housing demand.

To construct such a logistics plan for direct housing, it is crucial to characterize the uncertainty associated with housing demand stemming from disaster events, with a focus on hurricane disasters in this paper. In order to ensure a timely delivery of disaster housing units to victims, the logistics operation must be initiated shortly after the occurrence

*Corresponding author
shengyc@clemson.edu (S. Chen); yongjis@clemson.edu (Y. Song); dalbrig@clemson.edu (D. Albright); wpang@clemson.edu (W. Pang)
ORCID(s): 0000-0001-6839-522X (Y. Song)

of a disaster event, such as when a major hurricane makes landfall. The challenge is that only a rough estimation of the housing demand is available at that time. The actual demand information from victims, e.g., through FEMA's Individual Assistance (IA) program (FEMA, 2023), can take weeks or even months to collect. The discrepancy between estimated and actual demand data cannot be neglected, as it can lead to either over-preparation or under-preparation, either of which can incur substantial economic and social cost. For instance, FEMA purchased more MHUs than needed in Texas after Hurricane Harvey in 2017, leading to unnecessary expenditure of up to $152 million (Erwin, 2020). Conversely, the under-utilization of disaster housing assistance led to 11,000 families in emergency shelters for nearly six weeks after the storm during Hurricane Sandy in 2012 (By Ken Serrano, Asbury Park (N.J.) Press, 2012). Addressing the uncertain housing demand is critical to a timely and effective implementation of a disaster housing plan.

In this paper, we propose a data-driven decision-support framework that integrates disaster housing demand estimation into disaster housing logistics planning via a two-stage chance-constrained stochastic programming (TSCC) model. We construct a spatial regression model for estimating housing demand based on a selected number of independent variables related to both the hazard and socioeconomic factors, which is trained from historical demand data from past major hurricane events. This regression model is subsequently used to generate disaster housing demand scenarios, which are incorporated into the TSCC model as input data. This framework allows us to (i) address disaster housing logistics planning in the aftermath of a disaster event and (ii) achieve the balance between logistics operational cost and its robustness towards extreme disastrous situations by leveraging two operational modalities, an ordinary modality and an emergency modality (Liu, Küçükyavuz, and Luedtke, 2016), with the latter serving as a contingency plan for situations when the demand is unexpectedly high. For the emergency modality, we allow emergency acquisition decisions at the expense of a higher cost. Since the emergency modality should only be activated in the most extreme situations where an unexpectedly high demand is realized, the percentage of scenarios that an emergency modality can be activated among all scenarios is set to be a risk tolerance parameters that is specified by the decision maker, giving rise to a chance-constrained model.

The rest of the paper is organized as follows. In Section 2, we review relevant literature on disaster housing logistics planning and disaster relief problems solved by stochastic programming. In Section 3, we describe in detail the TSCC model and the methods employed for solving the model. In Section 4, we present a spatial regression model for estimating disaster housing demand, followed by our numerical results based on a case study on Hurricane Ian in Section 5. These results show the efficacy of the TSCC model in comparison to other models and offer insights into disaster housing logistics planning through a set of sensitivity analyses.

2. Literature Review

In this section, two relevant topics are reviewed. First, we provide a general literature review on disaster housing logistics planning. Then, we review stochastic programming models applied to the disaster relief problems most relevant to our research.

2.1. Literature on disaster housing research

Compared with the general topic of disaster relief, the literature on disaster housing research is rather limited, mostly due the data scarcity, policy complexity, among other complicating factors. Most of the literature focuses on disaster housing architecture design and disaster housing demand estimation, instead of their logistics planning that integrates the two, which is what we focus on in this paper.

The literature related to disaster housing architecture design emphasizes on how decision-making in housing design can lead to a potential impact on the process of disaster housing recovery. For example, Hendriks, Basso, Sposini, van Ewijk, and Jurkowska (2017); Patel and Hastak (2013) aim to identify a better disaster housing design, with the goal of reducing the vulnerability of individuals affected by disasters through a deeper understanding of the principles related to hazard-resistant construction. Moreover, Wagemann (2017) focuses on the development and evaluation of housing design strategies, Félix, Branco, and Feio (2013) explore permanent housing reconstruction, and Félix, Monteiro, Branco, Bologna, and Feio (2015) identify the main causes of issues in temporary housing units. Within our proposed framework, by evaluating the performances of disaster housing logistics planning with and without alternative disaster housing solutions, we can showcase the value of these alternative designs in comparison with the existing disaster housing solutions.

The literature related to disaster housing demand estimation, requirement, and fulfillment focuses on characterizing the correlation between key natural hazard factors, socioeconomic factors, and the post-disaster housing needs. Perrucci

and Baroud (2020) underscore the need for further research in proactive management, storage, sustainability, and community resilience to effectively enhance post-disaster temporary housing with simulation approach. El-Anwar and Chen (2016) conduct a similar study, employing an optimization model to quantify the specific needs and preferences of each displaced family and optimize housing decisions. Perrucci and Baroud (2021) employ simulation approaches to address key decision-making trade-offs associated with critical attributes of disaster housing, such as locations, structures, and costs to estimate the losses for disaster housing. We emphasize that the estimation of housing demand is just one facet of the overall logistical plan – it is important to take a holistic perspective on disaster housing logistics planning. In our proposed framework, we integrate disaster housing demand estimation into disaster housing logistics planning using an appropriate stochastic programming model.

2.2. Literature on disaster relief logistics

While the literature on the logistics planning for disaster housing specifically is limited, the literature on general disaster relief logistics spans a wide range of topics. This breadth arises from the extensive disaster relief supply chain network operated by FEMA and state emergency management agencies in the US (Vanajakumari, Kumar, and Gupta, 2016). Stochastic programming is frequently employed in disaster planning to address the uncertainty arising from the disaster. Existing stochastic programming models for disaster relief logistics planning have predominantly concentrated at the strategic level, utilizing two-stage stochastic programs.

In these two-stage stochastic programming models, strategic-level logistics decisions, such as relief supply pre-positioning and transportation capacity allocation, are modeled as the first-stage decisions prior to the realization of demand, and operational-level decisions such as the delivery of disaster relief commodities to the disaster victims are modeled as the second-stage decisions with the realized demand information. Alem, Clark, and Moreno (2016) introduce a two-stage stochastic network flow model aimed at enhancing emergency logistics in disaster relief. This model takes into account multiple factors, including budget allocation, fleet sizing, procurement, and varying lead times, and incorporates the application of risk measures. Paul and Zhang (2019) develop a two-stage stochastic programming model for hurricane preparedness. The goal of the model is to determine the location of distribution points, medical supply levels, and transportation capacity before the hurricane, and make transportation decisions after the hurricane. Also, Yang, Duque, and Morton (2022) introduce a two-stage stochastic programming model and apply it in a rolling-horizon fashion to optimize fuel supply chain operations so that emergency diesel fuel demand for power generation in a hurricane's immediate aftermath can be mitigated. Similar hurricane preparedness studies can be found in, e.g., Duran, Gutierrez, and Keskinocak (2011); Morrice, Cronin, Tanrisever, and Butler (2016); Rawls and Turnquist (2010); Salmerón and Apte (2010); Sanci and Daskin (2021); Pouraliakbari-Mamaghani, Saif, and Kamal (2023); Sütiçen, Batun, and Çelik (2023); Velasquez, Mayorga, and Özaltın (2020); Wang, Dong, and Hu (2021). Nevertheless, despite the abundance of literature exploring logistics decisions for general relief supplies, there is a lack of research addressing the logistical planning of disaster housing in the face of demand uncertainty.

We will model the disaster housing logistic planning as a TSCC optimization model. This model encompasses strategic-level logistics decisions while also incorporating emergency modality to address unforeseen high-demand situations. The decision to adopt a chance-constrained model stems from the associated high cost of activating the emergency modality contingency plan. It is essential to limit the chance that the emergency modality is activated to be no larger than a prescribed risk level. This is consistent with the national disaster relief and emergency response framework established by FEMA.

3. Problem Description

In this section, we introduce a TSCC model for disaster housing logistics planning in alignment with the current direct housing practices of FEMA (see Figure 1), following their established timeline (FEMA, 2020). After the activation of the Individuals and Households Program (IHP) following the Presidential disaster declaration to a major disaster event, FEMA will initiate an evaluation of its direct housing inventory and start the procurement of new direct housing if necessary from contracted producers based on the estimated housing demand. We incorporate this planning decision into the first stage of the two-stage model, where planning decisions on housing acquisition are made with predicted housing demand information to minimize the total expected logistics and social cost. Afterwards, it takes several weeks to several months for FEMA to acquire the actual demand data through direct housing requests from victims and subsequent approvals. FEMA then proceeds with delivering direct housing to those in need based on the actual demand data. This operational decision is integrated into the second stage of the two-stage model.

Figure 1: The Timeline of the Direct Disaster Housing Logistics Plan by FEMA.

To further enhance the adaptability and effectiveness of our proposed plan, especially in addressing scenarios with unexpectedly high demand, we consider two operational modalities for the second stage, the *ordinary modality* and the *emergency modality*. For the ordinary modality, all housing allocation decisions are made based on the housing acquisition decision in the first stage, and no emergency acquisition is permitted. For the emergency modality, we allow emergency acquisition decisions at the expense of a higher cost. Since the emergency modality should only be activated in the most extreme situations where an unexpectedly high demand is realized, we limit the chance that an emergency modality is activated among all scenarios to be under a given threshold, giving rise to a chance-constrained stochastic programming model, which we discuss next.

3.1. Two-stage Chance-constrained Stochastic Programming

We consider a logistics planning problem for direct disaster housing, which is mainly concerned about the planning decisions on disaster housing acquisition and staging shortly after a major hurricane makes landfall, and operational decisions on housing allocation after the disaster housing demand is realized. Motivated by the criticality of a timely delivery of disaster houses to victims, we propose a time-indexed formulation to model the problem as a multi-period supply chain network flow model. We assume for the baseline model that each time period corresponds to a single day for simplicity, but this definition can be made flexible as we discuss in Section 5. The entire planning horizon is specified by a set $\mathcal{T} = \{1, 2, ..., T-1, T\}$. In the two-stage model, the first stage comprises of time periods $\mathcal{T}_f = \{1, 2, \dots, T_f\} \subseteq \mathcal{T}$ and the second stage comprises of time periods $\mathcal{T}_s = \{T_f + 1, T_f + 2, \dots, T-1, T\} \subseteq \mathcal{T}$. Furthermore, we define set $\mathcal{T}_d = \{T_d, T_d + 1, \dots, T-1, T\} \subseteq \mathcal{T}_s$, where each $t \in \mathcal{T}_d$ represents a time period at which the deprivation cost will incur, as we discuss in more detail next.

Another crucial reason for integrating a time-indexed formulation into the model is to account for deprivation costs. Deprivation cost functions play an important role in disaster logistics planning, allowing for the quantification of human suffering in the aftermath of disasters over time (Pernett, Amaya, Arellana, and Cantillo, 2022). Another rationale for integrating deprivation costs into the logistics planning model is to capture the cost that victims incur due to the lack of emergency planning (Moreno, Alem, Ferreira, and Clark, 2018). In recent years, most research within the area of disaster relief logistics planning has incorporated deprivation costs, such as Moreno et al. (2018); Pérez-Rodríguez and Holguín-Veras (2016); Rivera-Royero, Galindo, and Yie-Pinedo (2016). Despite the large number of studies on deprivation costs for different goods or services, to the best of our knowledge there is no prior study on deriving the deprivation cost function for disaster housing. However, Holguín-Veras, Pérez, Jaller, Van Wassenhove, and Aros-Vera (2013) conclude that the solutions will be similar as long as the model's estimated deprivation cost function strictly dominates the true function. In the study, we adopt the deprivation cost function by adapting from the literature (Holguín-Veras, Amaya-Leal, Cantillo, Van Wassenhove, Aros-Vera, and Jaller, 2016).

We model the disaster housing logistics network as a supply chain network with three types of nodes: the supply nodes I, the transshipment nodes W, and the demand nodes J (see Figure 9 in Appendix D for an illustration). This network structure is commonly used for a generic disaster relief logistics setting, as can be found in, e.g., Alem et al. (2016); Paul and Zhang (2019); Siddig and Song (2022), etc. We consider a set H of different types of housing solutions that are currently adopted by FEMA, including travel trailers and manufactured housing units (MHUs).

To enhance the model's flexibility to incorporate any alternative disaster housing architecture designs, we configure the model to allow alternative housing solutions, which are referred to as the "Alternative Modular Houses" (AMHs). We assume that these AMHs have the flexibility to substitute any of the existing housing solutions, i.e., trailers and MHUs. In Section 4, we will demonstrate how even a modestly designed AMH can provide benefits to the underlying problem. We consider a set N of different types of AMHs. Each AMH, denoted by $n \in N$, has the capability to substitute existing housing solutions by utilizing a specific number of its own units and a specific assembly time. We

assume that the existing disaster houses and the ones made through the substitutions of the AMHs provide the same living condition for victims for simplicity in this work, although we acknowledge that the disaster victims' preferences play an important role in disaster housing allocation. We define set $P = H \cup N$ to include all types of disaster housing solutions.

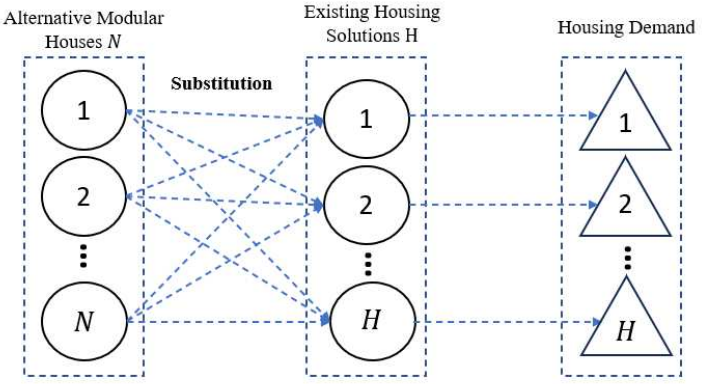

Figure 2: An illustration of the substitution of existing housing solutions by AMHs.

Finally, to incorporate the uncertainty in the disaster housing demand into our model, we consider a set of scenarios K, which are assumed to be equally likely for simplicity. Each scenario specifies a disaster housing demand realization for each of the demand nodes.

We are now ready to present the proposed TSCC model. We start with the parameter definition, followed by the definitions of decision variables and constraints, and finish with the complete formulation.

Parameters

$C_{i,w,p}$: unit transportation cost from supply node i to transshipment node w for type-p houses.

$C_{w,j,p}$: unit transportation cost from transshipment node w to victims in demand node j for type-p houses.

$O^F_{i,p}$: first-stage unit acquisition cost of type-p houses from supply node i.

$O^S_{i,p}$: second-stage unit acquisition cost of type-p houses from supply node i (under the emergency modality).

C^U_h: unit penalty cost incurred by unmet demand for type-h houses.

C^V_p: unit penalty cost incurred by unused inventory for type-p houses.

$C^D_{h,t}$: unit penalty cost incurred by deprivation of type-h houses for a deprivation time of t periods.

U_w: inventory capacity of transshipment node w.

u_p: amount of inventory level occupied by each type-p house.

E_i: number of production lines available at supply node i.

$\bar{E}_i$: number of extra production lines available for emergency modality at supply node i.

$D^k_{j,h}$: amount of demand of type-h houses in demand node j in scenario k.

λ_p: amount of transportation capacity levels occupied by each type-p house.

$\phi_{n,h}$: installation time of type-n AMH used to substitute an existing type-h house.

$B_{n,h}$: number of units of type-n AMH required to substitute an existing type-h house.

$V_{i,p}$: initial inventory level of type-p houses at supply node i.

$\tau_{i,p}/\bar{\tau}_{i,p}$: production time of type-p house in supply node i under the ordinary/emergency modality.

θ_i/θ_w: maximum number of housing units that can be sent from supply node i/transshipment node w within a single time period.

$\Delta_{i,w}$: number of time periods required for housing units to be shipped from supply node i to transshipment node w.

$\Delta_{w,j}$: number of time periods required for housing units to be shipped from transshipment node w to demand node j.

In our decision making framework, the first-stage problem determines the acquisition and staging decisions on disaster houses, while the second-stage problem focuses on the delivery decisions to the demand nodes under each scenario. We use the notation below for the decision variables:

First-stage decision variables

$x_{i,w,p,t}$: number of type-p houses sent from supply node $i \in I$ to transshipment node $w \in W$ at departure time t.

$s_{i,p,t}$: number of type-p houses started be manufactured from supply node i at time t.

$\mu_{w,p,t}$: inventory level of type-p houses in transshipment node w at time t.

$v_{i,p,t}$: inventory level of type-p houses at supply node i at time t.

$a_{i,t}$: number of production lines used by supply node i at the beginning of time t.

Second-stage decision variables (all associated with a scenario index k)

$f^k_{w,j,p,t}$: number of type-p houses sent from transshipment node w to demand node j at time t.

$f^k_{i,j,p,t}$: number of type-p houses sent from supply node i to demand node j at time t.

$f^{k,n}_{j,h,t}$: number of type-n AMHs starting to be assembled to substitute type $h \in H$ houses in demand node j at time t.

$\nu^k_{i,p,t}$: number of type-p houses started to be manufactured from supply node i at time t under the emergency modality.

$\ell^k_{i,j,p,t}$: number of type-p houses produced by supply node i for demand node j at time t under emergency modality.

$\mu^k_{w,p,t}$: inventory level of type-p houses in transshipment node w at time t.

$b^k_{i,t}$: number of extra production lines used by supply node i in the emergency modality at time t.

$q^k_{j,h,t}$: amount of unsatisfied housing demand at demand node j for type-h houses at time t.

As mentioned earlier, we provide two operational modalities for the second-stage problem, the ordinary modality and the emergency modality. Under the ordinary modality, the housing allocation decisions are made based on the first-stage acquisition and staging decisions, without the opportunity to make additional housing acquisitions after time $\mathcal{T}_f$. Under the emergency modality, the emergency acquisition and delivery are permitted after $\mathcal{T}_f$. For notational convenience, we denote $\mathbf{x} := (x, \mu, s, v)$ as the first-stage solution that is used as an input to the second-stage model, either with the ordinary modality or the emergency modality. Next, we present the formulations of the second-stage problem under the ordinary modality and the emergency modality, respectively.

Ordinary modality:

$$F_k(\mathbf{x}) = \min_y \sum_{w\in W}\sum_{j\in J}\sum_{t\in\mathcal{T}_s}\sum_{p\in P} C_{w,j,p} f^k_{w,j,p,t} + \sum_{j\in J}\sum_{h\in H} C^U_h q^k_{j,h,T} + \sum_{w\in W}\sum_{p\in P} C^V_p \mu^k_{w,p,T} + \sum_{j\in J}\sum_{t\in\mathcal{T}_d}\sum_{h\in H} C^D_{j,h,t} q^k_{j,h,t} \tag{1a}$$

$$\text{s.t. } \mu^k_{w,p,T_f} = \mu_{w,p,T_f},\ \forall w \in W,\ p \in P \tag{1b}$$

$$\mu^k_{w,p,t+1} + \sum_{j\in J} f^k_{w,j,p,t+1} = \sum_{i\in I} x_{i,w,p,t-\Delta_{i,w}} \mathbb{1}(t - \Delta_{i,w} \geq 1) + \mu^k_{w,p,t},$$
$$\forall w \in W,\ t = T_f, T_f + 1, \ldots, T-1,\ p \in P \tag{1c}$$

$$\sum_{j\in J}\sum_{p\in P} \lambda_p f^k_{w,j,p,t} \leq \theta_w,\ \forall t \in \mathcal{T}_s,\ w \in W \tag{1d}$$

$$\sum_{w\in W} f^k_{w,j,n,t} = \sum_{h\in H} f^{k,n}_{j,h,t+\phi_{n,j}},\ \forall t \in \mathcal{T}_s, j \in J,\ n \in N \tag{1e}$$

$$d^k_{j,h,t+1} = d^k_{j,h,t} + \sum_{n\in N} \frac{1}{B_{n,h}} f^{k,n}_{j,h,t-\phi_{n,h}} \mathbb{1}(t - \phi_{n,h} \geq T_f + 1)$$
$$+ \sum_{w\in W} f^k_{w,j,h,t-\Delta_{w,j}} \mathbb{1}(t - \Delta_{w,j} \geq T_f + 1),\ \forall j \in J,\ t \in \mathcal{T}_s \backslash \{T\},\ h \in H \tag{1f}$$

$$d^k_{j,h,t} + q^k_{j,h,t} = D^k_{j,h},\ \forall j \in J,\ h \in H,\ t \in \mathcal{T}_s \tag{1g}$$

$$f^{k,n}_{j,h,t} = 0,\ \text{if } t + \phi_{n,j} \geq T,\ \forall n \in N, j \in J, h \in H, t \in T \tag{1h}$$

$$f^k_{w,j,p,t} = 0,\ \text{if } t + \Delta_{w,j} \geq T,\ \forall w \in W, j \in J, p \in P, t \in T \tag{1i}$$

All variables are nonnegative

Emergency modality:

$$\bar{F}_k(\mathbf{x}) = \min_y \sum_{w\in W}\sum_{j\in J}\sum_{t\in\mathcal{T}_s}\sum_{p\in P} C_{w,j,p} f^k_{w,j,p,t} + \sum_{j\in J}\sum_{h\in H} C^U_h q^k_{j,h,T}$$
$$+ \sum_{w\in W}\sum_{p\in P} C^V_p \mu^k_{w,p,T} + \sum_{j\in J}\sum_{t\in\mathcal{T}_d}\sum_{h\in H} C^D_{j,h,t} q^k_{j,h,t}$$
$$+ \sum_{i\in I}\sum_{j\in J}\sum_{t\in\mathcal{T}_s}\sum_{p\in P} (O^S_{i,p} + C_{i,j,p}) f^k_{i,j,p,t} \tag{2a}$$

$$\text{s.t. (1b), (1c), (1g)} \tag{2b}$$

$$v^k_{i,p,T_f} = v_{i,p,T_f},\ \forall i \in I,\ p \in P \tag{2c}$$

$$v^k_{i,p,t+1} + \sum_{w\in W} x_{i,w,p,t+1} + \sum_{j\in j} f^k_{i,j,p,t+1}$$
$$= v^k_{i,p,t} + s_{i,p,t-\tau_{i,p}} \mathbb{1}(t - \tau_{i,p} \geq 1) + \nu^k_{i,p,t-\bar{\tau}_{i,p}} \mathbb{1}(t - \bar{\tau}_{i,p} \geq T_f + 1),$$
$$\forall i \in I,\ p \in P,\ t = T_f, T_f + 1, \ldots, T-1 \tag{2d}$$

$$\sum_{i\in I} f^k_{i,j,n,t-\Delta_{i,j}} \mathbb{1}(t - \Delta_{i,j} \geq T_f + 1) + \sum_{w\in W} f^k_{w,j,n,t-\Delta_{w,j}} \mathbb{1}(t - \Delta_{w,j} \geq T_f + 1)$$
$$= \sum_{h\in H} f^{k,n}_{j,h,t}, \forall j \in J,\ n \in N,\ t \in \mathcal{T}_s \tag{2e}$$

$$\forall j \in J,\ h \in H,\ t \in \mathcal{T}_s \tag{2f}$$

$$b^k_{i,T_f+1} = 0,\ \forall i \in I \tag{2g}$$

$$b^k_{i,t+1} + \sum_{p\in P} \nu^k_{i,p,t+1-\bar{\tau}_{i,p}} \mathbb{1}(t + 1 - \bar{\tau}_{i,p} \geq T_f + 1) = \sum_{p\in P} \nu^k_{i,p,t} + b^k_{i,t},\ \forall i \in I,\ t \in \mathcal{T}_s \tag{2h}$$

$$b^k_{i,t} \leq \bar{E}_i,\ \forall i \in I,\ t \in \mathcal{T}_s \tag{2i}$$

$$d^k_{j,h,t+1} = d^k_{j,h,t} + \sum_{n\in N} \frac{1}{B_{n,h}} f^{k,n}_{j,h,t-\phi_{n,h}} \mathbb{1}(t - \phi_{n,h} \geq T_f + 1)$$
$$+ \sum_{w\in W} f^k_{w,j,h,t-\Delta_{w,j}} \mathbb{1}(t - \Delta_{w,j} \geq T_f + 1) + \sum_{i\in I} f^k_{i,j,h,t-\Delta_{i,j}} \mathbb{1}(t - \Delta_{i,j} \geq T_f + 1),$$

$$\forall j \in J,\ t \in \mathcal{T}_s \backslash \{T\},\ h \in H \tag{2j}$$

$$f^k_{i,j,p,t} = 0,\ \text{if } t + \Delta_{i,j} \geq T, \forall i \in I, j \in J, p \in P, t \in T \tag{2k}$$

$$f^{k,n}_{j,h,t} = 0,\ \text{if } t + \phi_{n,j} \geq T,\ \forall n \in N, j \in J, h \in H, t \in T \tag{2l}$$

$$v^k_{i,p,t} = 0,\ \text{if } t + \bar{\tau}_{i,p} \geq T, \forall i \in I, p \in P, t \in T \tag{2m}$$

All variables are nonnegative.

The objective function (1a) minimizes the total cost of shipping, unmet demand penalty, unused inventory penalty, and deprivation penalty. Constraints (1b) establish the initial inventory of houses in the transshipment nodes at the beginning of the second stage, which equals to the inventory level of disaster housing units at the end of the first stage. Constraints (1c) ensure the balance constraints in the flow of houses delivered to victims (f) and houses procured from suppliers (x) in each transshipment node at each time t (see an illustration of the flow balance constraints in Figure 10a). At each time t, the number of the housings sent from the transshipment node is constrained by (1d). Since AMHs can be assembled to substitute any existing housing solutions $h \in H$, constraints (1e) model the assignment of the AMHs to serve the purpose of the existing houses. Constraints (1f) account for the number of houses received in each demand node at each time t (see an illustration in Figure 10b), and constraints (1g) restrict the total number of houses received in each demand node by time t to not exceed the actual demand by including unsatisfied housing demand variables q.

The emergency modality model is similar to the ordinary modality model, with three key distinctions: (i) we introduce an extra set of decision variables to capture the emergency acquisition decisions; (ii) since emergency acquisitions will change the inventory in the supply nodes, we employ v^k to monitor changes in the supply nodes inventory during the second stage instead of v. We also ensure a balance in the flow among the inventory v, first-stage decision x, emergency acquisition ν, and emergency delivery f via constraints (2d); and (iii) we have constraints (2i) and (2h) to model both the emergency acquisition and the production limits of supply nodes (see an illustration in Figure 10c).

The overall TSCC model:

Based on the two modalities defined above, the proposed TSCC model is given by:

$$\min \sum_{i\in I}\sum_{w\in W}\sum_{p\in P}\sum_{t\in\mathcal{T}}(O^F_{i,p} + C_{i,w,p})x_{i,w,p,t} + \frac{1}{|K|}\sum_{k\in K}\Big((1-z_k)F_k(\mathbf{x})) + z_k\bar{F}_k(\mathbf{x})\Big) \tag{3a}$$

$$\text{s.t.} \sum_{k\in K} z_k \leq \epsilon \cdot |K| \tag{3b}$$

$$v_{i,p,1} = V_{i,p},\ \forall i \in I, p \in P \tag{3c}$$

$$v_{i,p,t+1} + \sum_{w\in W} x_{i,w,p,t+1} = v_{i,p,t} + s_{i,p,t-\tau_{i,p}}\mathbb{1}(t - \tau_{i,p} \geq 1),\ \forall i \in I,\ \ p \in P,\ t \in \mathcal{T}\backslash\{T\} \tag{3d}$$

$$\sum_{w\in W}\sum_{p\in P}\lambda_p x_{i,w,p,t} \leq \theta_i,\ \forall t \in \mathcal{T}, i \in I \tag{3e}$$

$$\mu_{w,p,t+1} = \sum_{i\in I} x_{i,w,p,t-\Delta_{i,w}}\mathbb{1}(t - \Delta_{i,w} \geq 1) + \mu_{w,p,t}, \forall w \in W,\ t \in \mathcal{T}\backslash\{T\},\ p \in P \tag{3f}$$

$$\sum_{p\in P} u_p\mu_{w,p,t} \leq U_w,\ \forall w \in W,\ t \in \mathcal{T} \tag{3g}$$

$$a_{i,1} = 0,\ \forall i \in I \tag{3h}$$

$$a_{i,t+1} + \sum_{p\in P} s_{i,p,t+1-\tau_{i,p}}\mathbb{1}(t + 1 - \tau_{i,p} \geq 1) = \sum_{p\in P} s_{i,p,t} + a_{i,t}, \forall i \in I,\ t \in \mathcal{T}\backslash\{T\} \tag{3i}$$

$$a_{i,t} \leq E_i,\ \forall i \in I,\ t \in \mathcal{T} \tag{3j}$$

$$z_k \in \{0,1\},\ \forall k \in K$$

$$x_{i,w,p,t} = 0,\ \text{if } t + \Delta_{i,w} \geq T,\ \forall i \in I, w \in W, p \in P, t \in T \tag{3k}$$

$$s_{i,p,t} = 0,\ \text{if } t + \tau_{i,p} \geq T,\ \forall i \in I, p \in P, t \in T \tag{3l}$$

$$x_{i,w,p,t} \geq 0,\ \forall i \in I,\ w \in W,\ p \in P,\ t \in \mathcal{T}$$

The objective (3a) is to minimize the total expected cost, including both the first-stage and second-stage costs. Constraints (3d) maintain the flow balance in the inventory level v with the acquisitions s from supply nodes, and the delivered housing units x to demand points. The delivery capacity at any time t is bounded by constraints (3e). Constraints (3f) are used to keep track of the number of each house type present at the transshipment nodes during each time period t. These flow balance constraints are illustrated in Figure 10 in the Appendix. Additionally, (3g) incorporates the transshipment nodes' capacities. It is assumed that each production line has the capacity to produce only one house at a time. This restriction is enforced through the constraints specified in (3h) through (3j). In particular, (3i) tracks the number of production lines in use, and (3j) ensures that the total number of production lines being utilized at any given time t does not exceed the capacity E_i. (3b) limit the number of scenarios that the emergency modality can be activated, where ϵ is a user-specified risk tolerance parameter. We note that the relatively complete recourse property holds in our model – the inclusion of the decision variables representing demand shortages ensures that a feasible second-stage solution exists for any feasible first-stage solution.

Before we finish this subsection, we give a brief discussion on the *threshold-based* policy (Liu et al., 2016) provided by the TSCC model (3). The threshold-based policy is derived from the solution to the TSCC model associated with a given set of scenarios K, namely the *in-sample* scenarios. This policy can be applied to any demand realization, including scenarios that are not necessarily included in the scenario set K, namely the *out-of-sample* scenarios. Specifically, the threshold value v^* provides a guidance on whether or not the emergency modality should be activated for any demand realization, which is specified as: $v^* = \max_{k\in K}\{F_k(\mathbf{x}^*) : z_k = 0\}$, where $\mathbf{x}^*$ is an optimal first-stage solution to (3). In other words, when a decision maker executes the threshold-based policy for real-time operations, given any demand realization in the second stage, if the second-stage cost based on $\mathbf{x}^*$ under the ordinary modality exceeds v^*, then they will opt for the emergency modality; otherwise, they will operate under the ordinary modality.

3.2. Solution Approach

Solving formulation (3) directly by a commercial optimization solver, e.g., Gurobi, is unlikely to scale well as the number of scenarios $|K|$ increases. We apply a scenario decomposition framework for solving the TSCC model as outlined in Liu et al. (2016), while utilizing the optimality cuts introduced in Liu et al. (2016), Luedtke (2014) and Zeng, An, and Kuznia (2014). To begin, we define the master problem with a set of optimality cuts: $\theta \geq \alpha_\ell \mathbf{x} + \beta_\ell \mathbf{z} + \gamma_\ell, \forall \ell \in L$, used to approximate the second-stage value function, a set of scenarios K_0 that have the corresponding z variables set to 0, and a set of scenarios K_1 that have the corresponding z variables set to 1. Initially, $L = \emptyset$, $K_0 = \emptyset$ and $K_1 = \emptyset$ in (4).

$$M(K_0, K_1) = \min \sum_{i\in I}\sum_{w\in W}\sum_{p\in P}\sum_{t\in \mathcal{T}}(O^F_{i,p} + C_{i,w,p})x_{i,w,p,t} + \theta \tag{4a}$$

$$\text{s.t. Constraints (3c)} - \text{(3j)} \tag{4b}$$

$$\theta \geq \alpha_\ell \mathbf{x} + \beta_\ell \mathbf{z} + \gamma_\ell, \forall \ell \in L \tag{4c}$$

$$z_k = 0, k \in K_0 \tag{4d}$$

$$z_k = 1, k \in K_1 \tag{4e}$$

$$\text{all decision variables are nonnegative}$$

Next, we define the subproblems with a generic notation for the simplicity of presentation. For any given k, the corresponding subproblems for the ordinary modality plan and the emergency modality are defined as follows, with π_k and $\bar{\pi}_k$ being the corresponding dual variables, respectively:

$$(Ordinary) \min_{y_k \in R^{n_2}_+}\{Cy_k : Wy_k \geq h_k - T\hat{\mathbf{x}}\} = \max_{\pi_k}\{\pi_k(h_k - T\hat{\mathbf{x}}) : \pi W \leq C\} \tag{5}$$

$$(Emergency) \min_{\bar{y}_k \in R^{\bar{n}_2}_+}\{C\bar{y}_k : W\bar{y}_k \geq \bar{h}_k - T\hat{\mathbf{x}}\} = \max_{\bar{\pi}_k}\{\bar{\pi}_k(\bar{h}_k - T\hat{\mathbf{x}}) : \bar{\pi} W \leq C\} \tag{6}$$

The first set of optimality cuts are referred to as the big-M cuts (Luedtke, 2014). Given relaxation solution $(\hat{\mathbf{x}}, \hat{\mathbf{z}})$ where $\hat{\mathbf{z}} \in \{0,1\}^{|K|}$, we define two sets: $S(\hat{\mathbf{z}}) = \{k \in K : \hat{z}_k = 0\}$ and $\bar{S}(\hat{\mathbf{z}}) = K \backslash S(\hat{\mathbf{z}})$, and the big-M cut is given

by:

$$\theta + \sum_{k\in S(\hat{\mathbf{z}})} M_k z_k + \sum_{k\in \bar{S}(\hat{\mathbf{z}})} \bar{M}_k(1-z_k) \geq \frac{1}{|K|}\left(\sum_{k\in S(\hat{\mathbf{z}})} \pi_k(h_k - T\mathbf{x}) + \sum_{k\in \bar{S}(\hat{\mathbf{z}})} \bar{\pi}_k(\bar{h}_k - \bar{T}\mathbf{x})\right) \tag{7}$$

where M_k is a large enough number such that inequality (7) is redundant whenever $z_k = 1$ for some $k \in S(\hat{\mathbf{z}})$ or $z_k = 0$ for some $k \in \bar{S}(\hat{\mathbf{z}})$. To see its validity, for the given solution $(\hat{\mathbf{x}}, \hat{\mathbf{z}})$, this cut provide a lower bound on the second-stage cost. For any other integer feasible solution, we must have one $k \in S(\hat{\mathbf{z}})$ with $z_k = 1$ or $k \in \bar{S}(\hat{\mathbf{z}})$ with $z_k = 0$. Thus, with a large enough number M_k, inequality (7) is still valid.

Based on formulation (1) and (2), we can write the big-M cuts as follows, where the superscripts on the dual variables correspond to their respective constraint labels in formulation (1) and (2):

$$\begin{aligned}
&\theta + \sum_{k\in S(\hat{\mathbf{z}})} z_k M_k + \sum_{k\in \bar{S}(\hat{\mathbf{z}})} (1-z_k)\bar{M}_k \\
&\geq \frac{1}{|K|}\Bigg(\sum_{k\in S(\hat{\mathbf{z}})}\Bigg(\sum_{w\in W}\sum_{p\in P}\mu_{w,p,T_f}\pi^{(1b)}_{k,w,p} + \sum_{w\in W}\sum_{p\in P}\sum_{t\in\mathcal{T}_s}\Bigg(\sum_{i\in I} x_{i,w,p,t-\Delta_{i,w}}\mathbb{1}\left(t-\Delta_{i,w}\geq 1\right)\Bigg)\pi^{(1c)}_{k,w,t,p} \\
&\quad + \sum_{w\in W}\sum_{t\in\mathcal{T}_s}\theta_w\pi^{(1d)}_{k,w,t} + \sum_{t\in\mathcal{T}_s}\sum_{j\in J}\sum_{g\in G} D^k_{j,g}\pi^{(1g)}_{k,j,g}\Bigg) + \sum_{k\in\bar{S}(\hat{z})}\Bigg(\sum_{w\in W}\sum_{p\in P}\mu_{w,p,T_f}\bar{\pi}^{(1b)}_{k,w,p} \\
&\quad + \sum_{w\in W}\sum_{p\in P}\sum_{t\in\mathcal{T}_s}\Bigg(\sum_{i\in I} x_{i,w,p,t-\Delta_{i,w}}\mathbb{1}(t-\Delta_{i,w}\geq 1)\Bigg)\bar{\pi}^{(1c)}_{k,w,t,p} + \sum_{t\in\mathcal{T}_s}\sum_{j\in J}\sum_{g\in G}\bar{\pi}^{(1g)}_{k,j,g} D^k_{j,g} \\
&\quad + \sum_{i\in I}\sum_{p\in P} v^k_{i,p,T_f}\bar{\pi}^{(2c)}_{k,i,p} + \sum_{t\in\mathcal{T}_s}\sum_{p\in P}\sum_{i\in I}\Bigg(s_{i,p,t-\mathcal{T}_{i,p}}\mathbb{1}(t-\tau_{i,p}\geq 1) - \sum_{w\in W} x_{i,w,p,t+1}\Bigg)\bar{\pi}^{(2d)}_{k,i,t,p} \\
&\quad + \sum_{i\in I}\sum_{t\in\mathcal{T}_s}\bar{E}_i\bar{\pi}^{(2i)}_{k,i,t}\Bigg)\Bigg)
\end{aligned} \tag{8a}$$

The big-M parameters M_k and $\bar{M}_k$ need to be chosen to be sufficiently large. In Appendix A, we describe in detail how these parameters are chosen.

The second set of optimality cuts is referred to as the special cuts (Liu et al., 2016). Based on the generic notation of the subproblems shown in (5) and (6), the special cuts are given as follows (the validity follows from Theorem 1 in Liu et al. (2016)):

$$\begin{aligned}
\theta \geq &\frac{1}{|K|}\sum_{k\in S(\hat{\mathbf{z}})}\left(\pi_k(h_k - T\mathbf{x}) + (\min\{\pi_k h_k : k\in K\backslash S(\hat{\mathbf{z}})\} - \pi_k h_k)z_k\right) \\
&+ \frac{1}{|K|}\sum_{k\in\bar{S}(\hat{z})}\left(\bar{\pi}_k(\bar{h}_k - \bar{T}\mathbf{x}) + (\min\{\bar{\pi}_k h_k : k\in K\backslash\bar{S}(\hat{\mathbf{z}})\} - \bar{\pi}_k\bar{h}_k)(1-z_k)\right)
\end{aligned} \tag{9}$$

Based on (9), we can find that the special cut is similar to a big-M cut with specific big-M values where $\sum_{k\in S(\hat{\mathbf{z}})} z_k M_k = \sum_{k\in S(\hat{\mathbf{z}})}(\min\{\pi_k h_k : k\in K\backslash S(\hat{\mathbf{z}})\} - \pi_k h_k)z_k$ and $\sum_{k\in\bar{S}(\hat{\mathbf{z}})}(1-z_k)\bar{M}_k = (\min\{\bar{\pi}_k h_k : k\in K\backslash\bar{S}(\hat{\mathbf{z}})\} - \bar{\pi}_k\bar{h}_k)(1-z_k)$. The special cuts are shown to be stronger than the big-M cuts (Liu et al., 2016), which help accelerate the branch-and-bound procedure. However, more computational effort needs to be spent on generating these cuts compared to generating the big-M cuts: generating a special cut involves solving two subproblems, i.e., both the ordinary and emergency modalities, instead of only one that is involved in generating the big-M cuts.

The third set of optimality cuts is based on simple Benders cuts $\theta_k \geq \alpha_\ell\mathbf{x} + \gamma_\ell$ and $\bar{\theta}_k \geq \bar{\alpha}_\ell\mathbf{x} + \bar{\gamma}_\ell$ that lower approximate the value functions of the ordinary modality $F_k(\mathbf{x})$ and emergency modality $\bar{F}_k(\mathbf{x})$, respectively. Model (4) can then be written as:

$$M(K_0, K_1) = \min \sum_{i\in I}\sum_{w\in W}\sum_{p\in P}\sum_{t\in\mathcal{T}}(O^F_{i,p} + C_{i,w,p})x_{i,w,p,t} + \frac{1}{|K|}\sum_{k\in K}\left((1-z_k)\theta_k + z_k\bar{\theta}_k\right)$$

$$\text{s.t. Constraints (3c) - (3j)} \tag{10a}$$
$$\theta_k \geq \alpha_\ell \mathbf{x} + \gamma_\ell, \forall \ell \in L_k \tag{10b}$$
$$\bar{\theta}_k \geq \bar{\alpha}_\ell \mathbf{x} + \bar{\gamma}_\ell, \forall \ell \in \bar{L}_k \tag{10c}$$
$$z_k = 0, k \in K_0 \tag{10d}$$
$$z_k = 1, k \in K_1 \tag{10e}$$
$$\text{all decision variables are nonnegative}$$

Specifically, based on formulations (1) and (2), the Benders cuts $\theta_k \geq \alpha_\ell \mathbf{x} + \gamma_\ell$ and $\bar{\theta}_k \geq \bar{\alpha}_\ell \mathbf{x} + \bar{\gamma}_\ell$ can be written as follows:

$$\theta_k \geq \sum_{w\in W}\sum_{p\in P} \mu_{w,p,T_f} \pi^{(1b)}_{k,w,p} + \sum_{w\in W}\sum_{p\in P}\sum_{t\in\mathcal{T}_s} \left(\sum_{i\in I} x_{i,w,p,t-\Delta_{i,w}} \mathbb{1}\left(t - \Delta_{i,w} \geq 1\right) \right) \pi^{(1c)}_{k,w,t,p} \tag{11a}$$
$$+ \sum_{w\in W}\sum_{t\in\mathcal{T}_s} \theta_w \pi^{(1d)}_{k,w,t} + \sum_{t\in\mathcal{T}_s}\sum_{j\in J}\sum_{g\in G} D^k_{j,g} \pi^{(1g)}_{k,j,g}$$

$$\bar{\theta}_k \geq \sum_{w\in W}\sum_{p\in P} \mu_{w,p,T_f} \bar{\pi}^{(1b)}_{k,w,p} + \sum_{w\in W}\sum_{p\in P}\sum_{t\in\mathcal{T}_s} \left(\sum_{i\in I} x_{i,w,p,t-\Delta_{i,w}} \mathbb{1}(t - \Delta_{i,w} \geq 1) \right) \bar{\pi}^{(1c)}_{k,w,t,p} \tag{11b}$$
$$+ \sum_{t\in\mathcal{T}_s}\sum_{j\in J}\sum_{g\in G} \bar{\pi}^{(1g)}_{k,j,g} D^k_{j,g} + \sum_{i\in I}\sum_{p\in P} v^k_{i,p,T_f} \bar{\pi}^{(2c)}_{k,i,p}$$
$$+ \sum_{t\in\mathcal{T}_s}\sum_{p\in P}\sum_{i\in I} \left(s_{i,p,t-\mathcal{T}_{i,p}} \mathbb{1}(t - \tau_{i,p} \geq 1) - \sum_{w\in W} x_{i,w,p,t+1} \right) \bar{\pi}^{(2d)}_{k,i,t,p}$$

Model (10) involves bilinear terms in the objective function. These linear terms can be linearized using McCormick reformulations with big-M parameters or left to be handled directly by MIP solvers such as Gurobi. In our numerical experiment, we found that the latter option yielded better computational performance.

The complete details of the branch-and-cut decomposition algorithm for model (4) with big-M cuts and special cuts are shown in Algorithm 1 in Appendix A. The procedure is similar for the bilinear formulation (10) with Benders cuts (11).

4. Direct Temporary Disaster Housing Demand Estimation

In this section, we describe a spatial regression model for estimating housing demand data based on the disaster hazard conditions and socioeconomic factors, using available historical data collected from various sources. Specifically, we provide details of the data collection process in Section 4.1, and we describe the spatial regression model in Section 4.2.

4.1. Data Collection

Instead of estimating the housing demand quantity directly, we use the housing assistance rate (with respect to the total population) as the predictor, which is a normalized value that takes into account the potential number of direct housing assistance for trailers or MHUs. This rate is defined as the proportion of individuals in need of direct housing assistance for trailers or MHUs in relation to the total count of owner-occupied housing units.

As mentioned above, there are two categories of factors that have a significant impact on the number of individuals displaced (Deng, 2001), consequently influencing the housing assistance rate: (i) the prevailing natural hazard conditions, and (ii) the social vulnerability that quantifies the absence of necessary resilience to withstand the consequences of such hazards. In our experiments, we focus on hurricane disaster events and we consider high-water marks and the distance between the county and the hurricane's landfall point as predictive variables for assessing natural hazard conditions, following what is typically done in the literature (Davlasheridze and Miao, 2021). Unlike Davlasheridze and Miao (2021), we select the duration of sustained wind speeds rather than the maximum wind speed as our factor. This is because that the duration of wind storms above a threshold wind speed is recognized as a critical parameter for assessing damage and losses, as losses typically escalate with prolonged duration. This

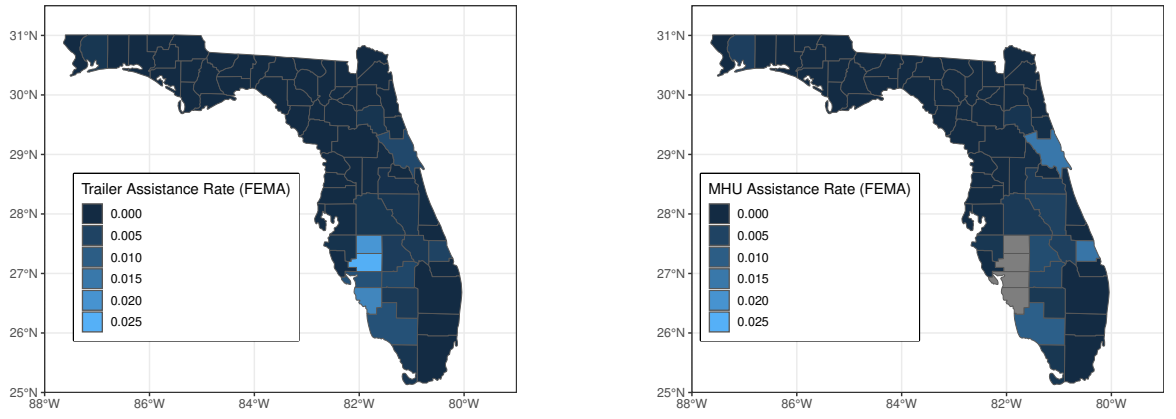

(a) Trailers (b) MHUs

Figure 3: Housing Assistance Rate Distribution from Hurricane Ian (regions shaded in gray have a housing assistance rate over 0.03).

phenomenon is attributable to the heightened peak pressures observed during longer durations, the susceptibility of various building components and cladding systems to diverse fatigue mechanisms, and the dependency of the yielding of linear elastic materials in the plastic range on the frequency of load cycles (Kopp, Li, and Hong, 2021). Hence, by integrating the duration of sustained wind speeds, we encompass not only the direct impact of wind speed on the housing but also the incorporation of diverse factors influencing the structural integrity of the housing. Thus, we opted to gather information on the total duration of sustained wind speeds during the hurricane passes surpassing the Saffir-Simpson category 3 threshold as our factor. Additionally, we have chosen the social vulnerability index (SVI) and population as our predictive variables for evaluating vulnerability and the insufficiency of resilience necessary to withstand these hazards.

We collected 265 county-level data points from eight recent major hurricane events, including Hurricane Florence, Harvey, Ida, Irma, Laura, Michael, Delta, and Sally. We determine the number of individuals requiring direct housing assistance for trailers and MHUs by extrapolating data from the OpenFEMA Dataset on major hurricanes, as the actual numbers of trailers and MHUs deployed for these disaster events are not publicly available to the best of our knowledge. This extrapolation is based on the financial aid disbursed through the Individual Assistance (IA) program (FEMA, 2023), taking the market prices of these disaster houses into account. Additionally, we gather data on the number of residents in owner-occupied housing units from the United States Census Bureau (U.S. Census Bureau., 2022). For the data on the aforementioned predicting factors, we collect: (i) the duration of sustained wind speeds in a county from NOAA's (National Oceanic and Atmospheric Administration) HURDAT2 database (National Oceanic and Atmospheric Administration., 2022), (ii) high-water marks from USGS's (U.S. Geological Survey) database (The United States Geological Survey., 2022), (iii) the distance between the county and the hurricane's point of landfall, (iv) social vulnerability index (SVI) from CDC (Center for Disease Control and Prevention) (The Centers for Disease Control and Prevention., 2020), which aggregates 16 social factors from United States Census Bureau, and (v) population. In the case of SVI, since SVI is published biennially, we calculate missing data by averaging the values from the previous and subsequent year.

4.2. Spatial Regression Models

We observe from historical data that the housing assistance rate for both trailers and MHUs is strongly correlated with that of its neighboring counties (see Figure 3 for an illustration for Hurricane Ian). Based on this observation, we perform Moran's I test (Moran, 1950) to capture the spatial autocorrelation in the dataset, which is given by:

$$I = \frac{n}{S_0} \frac{\sum_{i=1}^{n} \sum_{j=1}^{n} w_{i,j}(x_i - \bar{x})(x_j - \bar{x})}{\sum_{i=1}^{n}(x_i - \bar{x})^2}, \tag{12}$$

where x_i is a vector that represents the predicting factors associated with county $i = 1, 2, \ldots, n$, $w_{i,j}$ represents the spatial weight parameter, which corresponds to the distance between county i and j, calculated by the geodesic distance

based on their locations (we used the geographical center of each county to represent their location), and S_0 is the aggregate of all spatial weights:

$$S_0 = \sum_{i=1}^{n} \sum_{j=1}^{n} w_{i,j} \tag{13}$$

To compute Moran's I statistic, we must first create a distance weights matrix. To simplify the process, for each county, we opted to use the latitude and longitude of the geographical center of the county to represent the county's coordinates. Following the Moran's I test, the Moran's I statistic yielded values of 0.5055 for trailers and 0.4976 for MHUs. The p-value, found to be less than 10^{-16} for both trailer and MHU, allows us to reject the null hypothesis, indicating the existence of significant spatial autocorrelation in the housing assistance rate for both trailers and MHUs at a statistical confidence level of 0.05.

To proceed, we employed two distinct spatial models: the *spatial error model* and the *spatial lag model* (Anselin and Bera, 1998), for the trailer and MHU data, respectively. In both regression models, we employed a log transformation for the predictors and standardized the factors (to achieve better performance). Specifically, the spatial error model is given by :

$$y = X\beta + (I_n - \lambda W)^{-1}\epsilon, \tag{14}$$

where β is the regression coefficient vector, λ is the parameter indicating the intensity of spatial interdependency, W is the spatial weight matrix, where each entry w_{ij} is specified in the same way as (12), and ϵ is a multivariate normally distributed random variable, $\epsilon \sim N(0, \sigma^2 I)$, where I is the identity matrix.

Similarly, the spatial lag model is given by:

$$y = (I_n - \rho W)^{-1} X\beta + (I_n - \rho W)^{-1}\epsilon, \tag{15}$$

where β is the regression coefficient vector, ρ is the parameter indicating the intensity of spatial interdependency, and W and ϵ are defined in the same way as those in (14). For both models (14) and (15), we put together the predicting factor data x_i (as detailed in Section 4.1) for each county $i = 1, 2, \ldots, n$ as X, and the housing assistance rate data points as Y. We try to fit coefficients λ and β and coefficients ρ and β using W, X and Y, respectively.

We employed these two models to analyze the data, with different choices for the number of closest neighbors, which represents the spatial relationships between observations in space. We observe in our experiments that after applying a spatial regression model, the strong spatial correlation in the data is notably diminished for both trailers and MHU (see Figure 4). When the number of neighbors exceeds 4, the spatial correlation keeps at a similar level for both trailers and MHU. As a result, we choose a spatial regression model with the number of nearest neighbors set to be 4 in our experiments. The estimated housing assistance rate for both trailers and MHUs are shown in Figure 5.

5. Numerical Experiments

In this section, we present the experiment results of the proposed approaches via a case study based on Hurricane Ian 2022, with Florida (FL) being the study region. Hurricane Ian caused extensive damage, estimated to be between \$50 billion and \$65 billion damages, after its landfall in western FL with extreme winds and torrential rain. Mandatory evacuation orders were issued for parts of multiple counties. However, post-disaster disaster housing assistance was considered inefficient and delayed (Kimberly Kuizon, 2023). Our primary emphasis is placed on a county-level resolution, entailing the collection of county-level data or the aggregation of data into county-level data, as described in Section 4.

We start with Section 5.1 which outlines the process of constructing hurricane scenarios in our experiments using the spatial regression model described in Section 4. In Section 5.2, we describe the disaster housing data used in our experiments, including a specific type of AMH solution. Afterwards, we show how to apply our modeling and solution framework described in Section 3, and present computational results and sensitivity analyses on several key problem parameters.

5.1. Construction of Disaster Housing Demand Scenarios

To generate disaster housing demand scenarios for our case study based on Hurricane Ian, we collect data on the hurricane hazard conditions of Hurricane Ian and the socioeconomic data on the study region of FL at the county level.

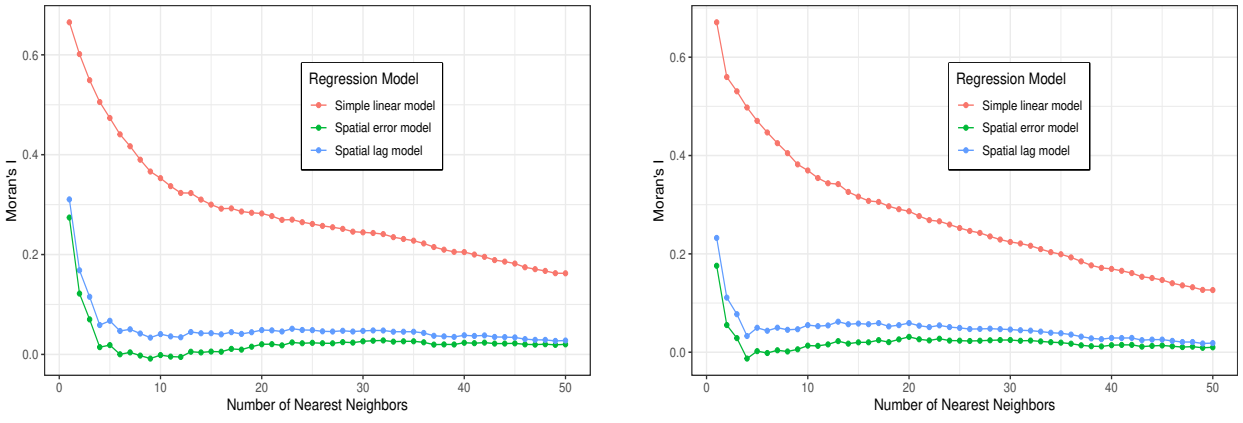

(a) Trailers (b) MHUs

Figure 4: Spatial Correlation in the Data Shown by Moran's I Test.

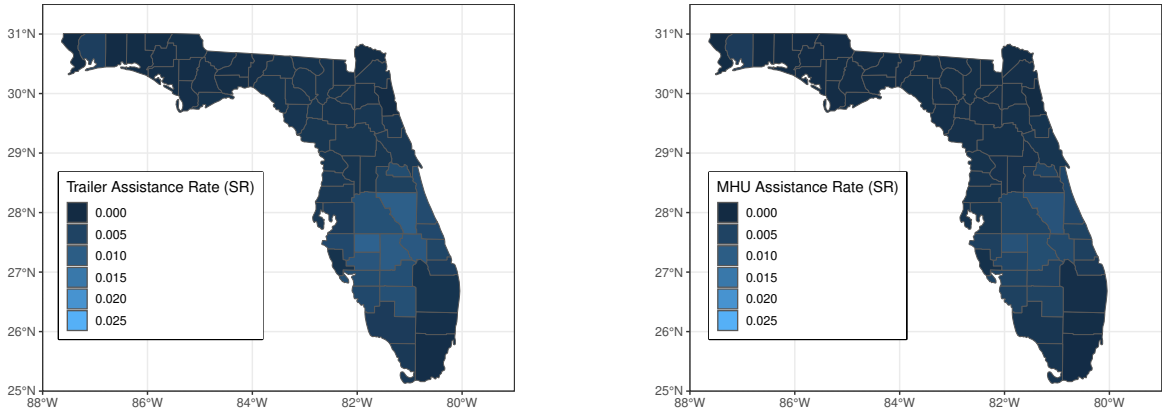

(a) Trailers (b) MHUs

Figure 5: Housing Assistance Rate Prediction for Hurricanes Ian.

We then generate disaster housing demand scenarios according to the spatial regression models shown in (14) and (15), by sampling from the probability distribution of the error term ϵ, which follows a normal distribution with mean of 0 and variance $\hat{\sigma}^2$.

The comparison between the mean predictions and the actual data is illustrated in Figure 5 and Figure 3. The mean squared error (MSE) of the mean prediction given by the spatial regression model is 0.0002 for the trailer and 0.0014 for the MHU. We have made a comparison of the spatial regression model with alternative prediction models, and the results will be shown in Section 5.5. While we can observe a discrepancy between our estimated value and the actual value in certain areas, the correlation coefficient reveals a positive association. Specifically, the Pearson correlation coefficient is 0.6052 for the trailer and 0.5247 for MHU. Additionally, the ranking of our estimated values aligns positively with the actual values, as indicated by the Spearman's rank correlation coefficients of 0.7519 for the trailer and 0.7668 for MHU. These results have shown the regression model's capability to capture the disaster housing demand to a certain degree.

5.2. Alternative Modular Housing Solutions

From a disaster housing design perspective, the proposed modeling and solution framework can serve as an optimization simulator capable of showing the value of any AMH designed for the disaster relief/recovery purpose. In the literature, numerous studies have delved into the design of post-disaster housing solutions (Hendriks et al.,

2017; John Squerciati, P.E, 2020; Patel and Hastak, 2013). However, these studies often lack an approximation of the potential reductions in social and logistical costs associated with implementing these new housing solutions. Here, our framework serves as a valuable tool for estimating both pre- and post-implementation of the values and costs in adopting an alternative modular housing (AMH) solution.

As a proof-of-concept for this effort, we include a specific type of AMH solution in our case study: a prototype unit from Liv-Connected (Liv for short) (Marissa Gluck., 2023). There are two reasons why Liv was chosen in the case study: (i) Liv is capable of replacing the trailer or MHU with the potential for expansion into a permanent house, and (ii) Liv is a modular house recommended as an alternative solution in the report by Texas General Land Office by Hagerty Consulting, Inc. (2020). When evaluating the capacities of a trailer, an MHU, and a Liv unit, we make the assumption that a single Liv unit can substitute a trailer, and two Liv units can equivalently substitute an MHU. In our experiments, we set the cost for a trailer to be $\$33,364$, and the cost for an MHU to be $\$73,735$, according to John Squerciati, P.E (2020). The cost information for Liv, as provided by Texas General Land Office by Hagerty Consulting, Inc. (2020), is presented in terms of cost per square foot. Consequently, we calculate the cost of a Liv's replacing a trailer or MHU by multiplying Liv's cost per square foot by the square footage of a trailer or MHU, which results in $\$47,940$ and $\$95,880$ respectively. We note that the cost estimated here is significantly different from the cost shown on Liv's website (Marissa Gluck., 2023). This is because the housing units that Liv proposed for disaster relief are considerably simpler than those showcased on the website, which are designed for the regular residence scenario. Solely focusing on the manufacturing process, the construction time of an MHU can range from two days to five weeks (Roy Diez., 2023). Here, we assume that trailer production takes less time than MHUs, with production rates set at 1/3 and 1/7 unit per day per production line, respectively. We set the production rate of a Liv unit to 1/7 units per day, based on the finding in Marissa Gluck. (2023) that the production time for a Liv unit is approximately one week, excluding the duration of the manufacturing drawings and some business processes. Additionally, Texas General Land Office by Hagerty Consulting, Inc. (2020) states that once the supply chain and factory are established, up to 250 units can be produced per month. By combining the production rate of a Liv unit with the monthly production capacity, we deduce that there are approximately 60 production lines and we use this data in our baseline instance. Finally, the Liv units require an additional three days for installation after delivery, while trailers and MHUs do not require any installation time.

5.3. Disaster Housing Logistics Network Construction and Problem Setting

To establish the logistics network for direct temporary disaster housing, we first construct three types of nodes in the supply chain network as defined in Section 3.1: The set of supply nodes I, the transshipment nodes W, and the demand nodes J. Due to the limited information on the actual logistics network operated and managed by FEMA, we construct a realistic logistics network based on our best estimate from relevant information in publicly available data source. Specifically, we selected nine locations as the supply nodes, including two designated permanent storage sites (Selma, AL, and Cumberland, MD), and six FEMA advance contractors as detailed in Erwin (2020); FEMA (2023). Under normal circumstances, the housing units produced by the contractors will be stored in the permanent storage sites. In the event of a disaster, the houses will be relocated from the permanent storage sites to temporary storage sites near the affected areas, and FEMA may acquire additional housing units from the contractors. Consequently, we selected the two permanent storage sites as suppliers with inventory but without production capability, and the six contractors are considered suppliers with certain production capability but zero starting inventory. For the transshipment nodes, one location was randomly picked from FL's boundary inland, which is appropriate for our purpose as deliveries can reach any county within a single time period (a day) from any point in Florida. For the demand nodes, all counties in FL were selected. The distances between locations were calculated using the Google Map API, and the unit transportation cost (per mile) was set to be $\$10$. For the deprivation cost function, we follow the function $y = 0.9814e^{0.0188x}$ from the literature (Holguín-Veras et al., 2016), where x represents the number of days delayed, and y represents the deprivation cost factor. We compute the deprivation cost by multiplying the deprivation cost factor by a base cost, which is chosen to be $1/120$ of the cost of the demanded housing type, where the maximum deprivation cost that a victim can incur is approximately 120 times the base cost, given by $\sum_{x=1}^{T_d} 0.9814e^{0.0188x}$. The guiding assumption here is that the maximum deprivation cost for a victim, i.e., the demand is fulfilled at the end of the planning horizon, is equivalent to the cost of the demanded housing type. For the unmet penalty cost, we set the unit of unmet penalty cost as five times of the cost of the demanded housing type in the baseline instance. Following FEMA's current practice, which allows for the re-utilization of housing in the subsequent disaster events, the incurred additional expense for the unused units merely entails their return to the permanent staging areas. We thus choose the unmet penalty cost to be 0.05 times the

housing price, representing the average transportation cost from staging area to permanent staging areas. The housing inventory and production rate information is collected from FEMA (2018). In addition, FEMA checks if the units in the inventory meet their standard before delivery. According to FEMA (2018), there are approximately 1,250 mobile homes, but only 630 passed quality and cleaning inspections for delivery. Therefore, we conduct a sensitivity analysis in Appendix C on different initial inventory levels to provide a more realistic assessment.

5.4. Experiment Results

We implemented the proposed model and solution approaches in Python, using Gurobi 10.0 as the optimization solver with the computational time limit set to be four hours. All experimental results were obtained utilizing a compute node sourced from the Palmetto Cluster Clemson University (2024) with a 48GB RAM, 2.10GHz CPU, one thread per core and 96 cores per socket configuration. First, we present in Section 5.4.1 the computational performances of the proposed time-indexed model. Subsequently, we present the performance of an out-of-sample stability test in Section 5.4.2 focusing on the resulting threshold policy obtained from solving the TSCC model. Finally, we compare the performances of the proposed TSCC model with alternative approaches in Section 5.4.3.

5.4.1. Computational Performance Enhancements

In our preliminary experiment results using using the special cuts and big-M cuts with model (4), we observe that when the number of scenarios $|K|$ is large, no feasible solution can be produced within the time limit of four hours. This motivated us to develop the following heuristic approach to provide an initial feasible solution. The idea of the heuristic approach is that, given a preparation decision $\widetilde{x}$, the activation of emergency modality will prioritize scenarios that have the greatest benefit from activating it. Equivalently, it will assign to scenarios having the most substantial decrease in cost upon activating the emergency modality, which is given by $F_k(\widetilde{x}) - \bar{F}_k(\widetilde{x})$ for each scenario k. Based on the observation, in the absence of an appropriate preparation decision $\widetilde{x}$, we estimate the decrease in cost resulting from activating the emergency modality for each scenario by assigning each scenario with the corresponding perfect-information preparation decisions. Specifically, first, we solve a combined problem that includes both the first- and second-stage problem for each scenario under both the ordinary and emergency modalities. This is equivalent to solving model (3) with a single scenario at a time with either ordinary and emergency modality, while excluding the constraint (3b). The two solutions that we obtain from each scenario, one for the ordinary modality and the other for the emergency modality, are used to assign the z values in the following heuristic way: we set $z_k = 1$ to the top $\epsilon|K|$ scenarios with the greatest cost differences between ordinary and emergency modality solutions, and set $z_k = 0$ for all other scenarios. Then, we re-solve model (3) with this fixed z to obtain an initial heuristic solution, which is a two-stage stochastic linear program. When $|K| \geq 20$, this model becomes too large for Gurobi to handle, necessitating the utilization of the branch-and-cut decomposition algorithm for solving this two-stage model. The cuts generated during this branch-and-cut procedure can be preserved and later added as valid inequalities into the original TSCC model (3). Consequently, when solving the original model (3), we benefit not only from an initial heuristic feasible solution but also some optimality cut information derived from generating the heuristic solution.

In Table 1, we show the general computational performance on the branch-and-cut algorithm with and without the initial feasible solution obtained by this simple heuristics, across various values of $|K|$ ($|K| = 20, 50, 100$) and ϵ ($\epsilon = 5\%, 10\%$) and different types of cuts. We use the following abbreviations for the column titles: (i) **Approach**: "Spec+BigM with (4)" represents the approach using model (4) with both the special cuts and big-M cuts, "Spec+Benders with (10)" represents the approach using model (10) with both the special cuts and Benders cuts, and "Benders with (10)" represents the approach using model (10) with only the Benders cuts. (ii) **Initial Heuristic**: "Heur" represents the setting where the heuristic solution described above is provided as an initial feasible solution, while "Heur+Cuts" represents the setting where both the initial solution and the cuts generated through the process of generating this solution are included for the TSCC model; (iii) **Heuristic Time**: the percentage of the total time spent on finding the initial heuristic solution; (iv) **Big-M Cut Time**, **Special Cut Time** and **Benders Cut Time**: the proportion of overall time dedicated to generating big-M cuts, special cuts and Benders cuts, respectively (Note that the Special Cut Time here does not include the time spent solving additional subproblems.); (v) **Subproblem Total Time**: the proportion of total time expended on solving the subproblems; (vi) **Time per Subproblem**: the average time to solve a single subproblem. In addition, we use "TL" to indicate that the total runtime hits the time limit of four hours, and we use "∞" to denote the case when a feasible solution is not found by the time limit.

From Table 1, it is evident that solely offering an initial heuristic solution may not have benefits across all instances with small $|K|$. However, the incorporating initial heuristic solution becomes critical for dealing with instances with

|K|	ϵ	Approach	Initial Heuristic	Heuristic Time	Optimality Gap	Total Time	Big-M Cut Time	Special Cut Time	Benders Cut Time	Subproblem Total Time	Time Per Subproblem
20	5%	Spec + BigM with (4)	-	-	0%	1221	5.2%	3.3%	0.0%	91.2%	0.12
			Heur	34%	0%	690	5.1%	3.3%	0.0%	91.2%	0.12
			Heur+Cuts	38%	0%	637	5.3%	3.3%	0.0%	91.0%	0.12
		Spec + Benders with (10)	-	-	0%	265	0.0%	3.4%	3.0%	94.3%	0.11
			Heur	58%	0%	219	0.0%	4.3%	1.1%	93.5%	0.11
			Heur+Cuts	59%	0%	221	0.0%	3.3%	2.2%	94.5%	0.11
		Benders with (10)	-	-	0%	168	0.0%	0.0%	2.4%	96.5%	0.10
			Heur	63%	0%	199	0.0%	0.0%	4.1%	94.0%	0.11
			Heur+Cuts	59%	0%	209	0.0%	0.0%	3.5%	95.6%	0.10
	10%	Spec + BigM with (4)	-	-	0%	4101	5.4%	3.5%	0.0%	91.0%	0.10
			Heur	15%	0%	1999	5.7%	3.7%	0.0%	90.5%	0.10
			Heur+Cuts	14%	0%	2143	5.9%	3.8%	0.0%	90.3%	0.10
		Spec + Benders with (10)	-	-	0%	228	0.0%	3.6%	2.3%	93.8%	0.11
			Heur	57%	0%	178	0.0%	3.5%	2.5%	93.1%	0.10
			Heur+Cuts	56%	0%	178	0.0%	3.3%	2.0%	94.3%	0.10
		Benders with (10)	-	-	0%	124	0.0%	0.0%	3.8%	95.7%	0.14
			Heur	61%	0%	128	0.0%	0.0%	7.9%	91.3%	0.11
			Heur+Cuts	60%	0%	118	0.0%	0.0%	5.0%	94.0%	0.10
50	5%	Spec + BigM with (4)	-	-	0%	TL	5.3%	3.3%	0.0%	91.5%	0.12
			Heur	6%	0%	13640	5.2%	3.3%	0.0%	91.4%	0.12
			Heur+Cuts	6%	0%	TL	5.4%	3.4%	0.0%	93.6%	0.12
		Spec + Benders with (10)	-	-	0%	1198	0.0%	1.4%	3.2%	95.1%	0.11
			Heur	31%	0%	1013	0.0%	3.4%	1.6%	94.6%	0.12
			Heur+Cuts	19%	0%	1623	0.0%	3.3%	1.0%	95.5%	0.11
		Benders with (10)	-	-	0%	560	0.0%	0.0%	1.6%	98.0%	0.10
			Heur	19%	0%	1101	0.0%	0.0%	1.4%	97.5%	0.10
			Heur+Cuts	31%	0%	678	0.0%	0.0%	1.8%	97.6%	0.10
	10%	Spec + BigM with (4)	-	-	∞	TL	5.7%	3.7%	0.0%	91.9%	0.10
			Heur	6%	8%	TL	6.0%	3.9%	0.0%	91.7%	0.10
			Heur+Cuts	6%	8%	TL	6.1%	3.8%	0.0%	92.4%	0.10
		Spec + Benders with (10)	-	-	0%	354	0.0%	3.2%	2.0%	91.5%	0.10
			Heur	43%	0%	589	0.0%	3.0%	1.9%	86.8%	0.10
			Heur+Cuts	54%	0%	447	0.0%	3.0%	2.0%	89.5%	0.10
		Benders with (10)	-	-	0%	314	0.0%	0.0%	2.5%	70.8%	0.10
			Heur	36%	0%	540	0.0%	0.0%	2.4%	71.7%	0.10
			Heur+Cuts	33%	0%	574	0.0%	0.0%	2.2%	77.4%	0.10
100	5%	Spec + BigM with (4)	-	-	∞	TL	5.5%	3.5%	0.0%	94.0%	0.12
			Heur	10%	6%	TL	5.5%	3.5%	0.0%	93.4%	0.12
			Heur+Cuts	10%	6%	TL	5.7%	3.5%	0.0%	91.4%	0.10
		Spec + Benders with (10)	-	-	0%	3039	0.0%	2.6%	0.7%	79.2%	0.10
			Heur	15%	0%	4367	0.0%	2.1%	0.8%	66.8%	0.10
			Heur+Cuts	27%	0%	2343	0.0%	3.0%	1.0%	87.8%	0.10
		Benders with (10)	-	-	7%	TL	0.0%	0.0%	0.1%	4.9%	0.10
			Heur	3%	9%	TL	0.0%	0.0%	0.1%	5.1%	0.10
			Heur+Cuts	3%	10%	TL	0.0%	0.0%	0.1%	6.0%	0.10
	10%	Spec + BigM with (4)	-	-	∞	TL	5.7%	3.6%	0.0%	91.1%	0.10
			Heur	13%	12%	TL	6.0%	3.8%	0.0%	92.0%	0.10
			Heur+Cuts	13%	9%	TL	5.7%	3.7%	0.0%	91.9%	0.12
		Spec + Benders with (10)	-	-	6%	TL	0.0%	0.4%	0.1%	10.1%	0.10
			Heur	4%	5%	TL	0.0%	0.2%	0.1%	5.3%	0.10
			Heur+Cuts	4%	5%	TL	0.0%	0.2%	0.1%	4.9%	0.09
		Benders with (10)	-	-	60%	TL	0.0%	0.0%	0.1%	4.9%	0.10
			Heur	2%	58%	TL	0.0%	0.0%	0.1%	4.8%	0.10
			Heur+Cuts	2%	59%	TL	0.0%	0.0%	0.1%	3.5%	0.10

Table 1
Computational Performances for Various Approaches and Initial Heuristics Settings.

larger $|K|$, which are more challenging instances, in reducing the optimality gap within time limits. Additionally, while providing only an initial heuristic solution may not be advantageous, incorporating cuts generated through getting initial heuristic solution as extra constraints appears to help reduce the computational time.

In addition, when $|K| \leq 50$, we observe that Benders with (10) yields significantly competitive results than Spec + BigM with (4) and Spec + Benders with (10). However, this is not the case for $|K| = 100$: Spec + Benders with (10) becomes more effective. While using Spec + BigM with (4), we note that the computational challenge in the branch-and-cut algorithm stems from the long computational time for solving the subproblems in all the cases, irrespective of the presence of an initial heuristic solution, which accounts for approximately 90% to 94% of the total time. On the other hand, for Benders with (10), this is the case when $|K| \leq 50$, but the time spent on solving the subproblems is only attributed to approximately 3% to 6% of the total computational time when $|K| = 100$. This indicates that the computational challenge in these settings shifts from solving the subproblems to solving the master problems, possibly

Approach	(|K|,e)	TIU	Total Cost	Heuristic Gap	Total Time	Coarse Model Optimality Gap	Coarse Model Time	Refinement Time	First-stage Cost	Subproblem Time	# of B&B Nodes	Time Per Subproblem
Spec + BigM with (4)	(20,5%)	1	796038		690	0%	690	0	71%	413	95	0.11
		2	832703	5%	604	0%	593	11	60%	415	202	0.05
		3	858128	8%	557	0%	536	21	55%	339	267	0.03
		4	956498	20%	504	0%	479	25	44%	340	374	0.02
	(20,10%)	1	779400		1999	0%	1999	0	72%	1535	412	0.09
		2	813383	4%	1470	0%	1460	10	62%	1198	600	0.05
		3	836239	7%	1182	0%	1167	15	56%	937	733	0.03
		4	920184	18%	1275	0%	1253	22	43%	954	1029	0.02
	(50,5%)	1	843992		13640	0%	13640	0	67%	11690	1074	0.11
		2	892887	6%	6276	0%	6217	59	56%	5264	1004	0.05
		3	928164	10%	13855	0%	13785	70	51%	12009	3752	0.03
		4	1024094	21%	7175	0%	7089	86	39%	5970	2674	0.02
	(50,10%)	1	821628		TL	8%	TL	0	69%	13209	1328	0.10
		2	864457	5%	TL	5%	TL	52	58%	12960	2609	0.05
		3	896096	9%	TL	5%	TL	67	52%	12752	4065	0.03
		4	984760	20%	TL	3%	TL	87	41%	12682	5545	0.02
	(100,5%)	1	865009		TL	6%	TL	0	65%	13451	619	0.11
		2	918879	6%	TL	4%	TL	56	55%	13118	1295	0.05
		3	957538	11%	TL	4%	TL	76	49%	12938	2044	0.03
		4	1053353	22%	TL	3%	TL	140	38%	12709	2753	0.02
	(100,10%)	1	842646		TL	12%	TL	0	67%	13242	689	0.10
		2	894172	6%	TL	7%	TL	146	56%	13038	1273	0.05
		3	929918	10%	TL	7%	TL	126	51%	12835	2005	0.03
		4	1019845	21%	TL	6%	TL	192	39%	12796	2810	0.02
Spec + Benders with (10)	(20,5%)	1	796038		219	0%	219	0	71%	87	21	0.10
		2	832703	5%	93	0%	93	2	60%	33	20	0.04
		3	858128	8%	71	0%	71	2	55%	35	27	0.03
		4	956498	20%	60	0%	60	2	44%	31	35	0.02
	(20,10%)	1	779400		178	0%	178	0	72%	70	18	0.10
		2	813383	4%	113	0%	113	2	62%	56	29	0.05
		3	836239	7%	77	0%	77	3	56%	39	30	0.03
		4	920184	18%	48	0%	48	4	43%	21	24	0.02
	(50,5%)	1	843992		1013	0%	1013	0	67%	665	60	0.11
		2	892887	6%	355	0%	355	2	56%	216	44	0.05
		3	928164	10%	282	0%	282	7	51%	182	58	0.03
		4	1024094	21%	146	0%	146	7	39%	75	35	0.02
	(50,10%)	1	817715		589	0%	589	0	69%	292	31	0.09
		2	859708	5%	312	0%	312	7	58%	132	31	0.04
		3	897099	10%	365	0%	365	7	52%	129	45	0.03
		4	993397	21%	393	0%	393	14	40%	98	48	0.02
	(100,5%)	1	865000		4367	0%	4367	0	65%	2490	125	0.12
		2	917929	6%	13654	0%	13654	14	55%	366	42	0.04
		3	963013	11%	7785	0%	7785	14	49%	485	87	0.03
		4	1067434	23%	4908	0%	4908	14	38%	280	66	0.02
	(100,10%)	1	842597		TL	5%	TL	0	67%	758	40	0.12
		2	889503	6%	TL	6%	TL	6	56%	369	45	0.04
		3	930799	10%	TL	4%	TL	14	51%	251	42	0.03
		4	1028384	22%	TL	4%	TL	14	39%	263	70	0.02

Table 2
Computational Performance of the Time Period Coarsening Heuristic Approach.

due to the existence of bilinear terms in the objective function of (10). Furthermore, when $|K| = 100$, Benders with (10) resulted in a stronger upper bound but a much weaker lower bound compared to Spec + BigM with (4). In this case, Spec + Benders with (10) appears to leverage the advantages of both Benders with (10) and Spec + BigM with (4), yielding better computational results by effectively balancing the time required to solve the subproblem and the master problem.

A heuristic approach based on time period coarsening Motivated by instances and approaches where the primary computational challenge stems from the time spent on solving the subproblems, we propose a heuristic solution approach based on coarsening the definition of a time period from one day per period to $\psi > 1$ days per period. Under the transition, the first-stage encompasses time periods $\mathcal{T}_f^\psi = \left\{1, 2, \ldots, \lfloor \frac{T_f}{\psi} \rfloor\right\}$, while the second-stage comprises time periods $\mathcal{T}_s^\psi = \left\{\lfloor \frac{T_f}{\psi} \rfloor + 1, \lfloor \frac{T_f}{\psi} \rfloor + 2, \ldots, \lfloor \frac{T}{\psi} \rfloor\right\}$. As a result, the entire planning horizon is truncated into $\mathcal{T}^\psi = \mathcal{T}_f^\psi \cup \mathcal{T}_s^\psi$. To accommodate the coarsened time period definition, the following parameters require adjustments by multiplication with ψ: the inventory capacity of the staging area (U), the unit capacity in a delivery (λ), and the number of production lines (E). On the other hand, the following parameters necessitate modification through division by ψ: the installation time for building an AMH (ϕ) and the production time (τ). Additionally, the input for the deprivation cost function should be adapted to ψt. While the solution derived from the coarse time period $\psi > 1$ model may be infeasible for the original model due to the necessary adjustments made to align with the coarsened time period definition, it provides an upper limit on the delivery flow for every ϕ time periods. With this information, we

can refine the solution of the model with coarsened time periods to find a feasible solution of the original model, by solving the original model with the flow limitation constraints and the fixed z values from the model with coarsened time periods.

Table 2 presents the results regarding the impact of time period coarsening on computational time, cost structure and the solution quality. In this table, we use the following abbreviations for the column titles: (i) **Approach**: "Spec+BigM with (4)" represents the approach using model (4) with both the special cuts and big-M cuts, and "Spec+Benders with (10)" represents the approach using model (10) with both the special cuts and Benders cuts; (ii) **TIU**: the time coarsening factor ψ; (iii) **Heuristic Gap**: the percentage increase in the total cost by the coarsened model compared to the original model (with $\psi = 1$); (iv) **Coarse Model Optimality Gap**: the optimality gap achieved by the coarsened model; (v) **Coarse Model Time** and Refinement Time: the time taken for solving the coarsened model and for the solution refinement process described above, respectively; (vi) **Total Time**: the overall computational time; (vii) **Subproblem Time**: the total time spent to solve subproblems; (viii) **# of B&B Nodes**: the total number of B&B nodes explored by the branch-and-cut algorithm for the coarsened model. The experiments are conducted with an initial feasible solution constructed based on the proposed heuristic approach, as this setting offers the best overall computational performance according to Table 1.

In Table 2, for solving the model with coarsened time periods, we can see that although it remains evident that the percentage of time spent solving subproblem is still similar to Table 1, there has been a notable decrease in the time spent on solving subproblems due to the coarsened time periods. Consequently, this allows the algorithm to explore more nodes within the branch-and-bound tree, resulting in an enhanced performance. In the instances that are solved to optimality (i.e., with a 0% optimality gap) within the time limit, the overall solution time by the model with coarsened time periods can be significantly reduced. For instances not solved to optimality within the time limit using Spec + BigM with (4), the number of nodes explored in the branch-and-bound algorithm is between 2 to 4 times larger than that of the original problem. Moreover, the computational efficiency improvements do not largely compromise solution quality. Compared to the total cost of the original model, setting $\psi = 2, 3$, and 4 incurs a 5%, 8%, and 21% increase on average, respectively. This shows the effectiveness of the proposed time period coarsening heuristic approach in achieving the balance between computational time and solution quality using approach Spec + BigM with (4). On the other hand, we see that although the same observation can be made in applying this time period coarsening heuristic to Spec + Benders with (10) for instances with $|K| \leq 50$, for larger instances (when $|K| = 100$), the effectiveness of this heuristic is relatively insignificant.

5.4.2. Solution Stability

We investigate the out-of-sample solution stability on the number of scenarios $|K|$ based on the threshold-based policy provided by the TSCC model (Liu et al., 2016), which is explained in Section 3.1. Recall that the threshold-based policy is derived from the solution to the TSCC model associated with a given set of scenarios K. Given that solving the TSCC with different numbers of scenarios $|K|$ yields distinct threshold values of υ^*, it is imperative to have a sufficient number of scenarios to ensure the stability of the resulting threshold-based policy, which is specified by value υ^*. In this experiment, we utilize the first-stage solution $\mathbf{x}^*$ and derive the threshold υ^* from various $(|K|, \epsilon)$ settings, and test their out-of-sample performance under an out-of-sample size of 1000 scenarios. For each sample size $|K|$, we conduct 10 replications and a threshold value υ^* for each replication. By computing the percentage of emergency modality activation within this set of out-of-sample scenarios, which is denoted as $\hat{\epsilon}$, with the original ϵ values, we can assess the corresponding solution stability in each setting. We note that the $\hat{\epsilon}$ values are computed by the average over the 10 replications.

The solution stability results on the threshold-based policy are presented in Figure 6 and Figure 7. In Figure 6, the x-axis and y-axis represent the ϵ value used in the TSCC model and the $\hat{\epsilon}$ value derived from the out-of-sample experiment, respectively. Here, we observe that when $|K| = 100$, the corresponding dashed line closely aligns with the black line, whereas a considerable amount of deviation is observed when $|K|$ is smaller. This indicates that a satisfactory level of solution stability can be achieved when $|K| = 100$ in our test instances. In Figure 7, we show the out-of-sample performance of the threshold-based policy on more detail, each subfigure depicting a specific $(|K|, \epsilon)$ setting. The x-axis and y-axis denote the operational cost of a scenario and its frequency (among the 1000 out-of-sample scenarios), respectively. The solid line and dashed line represent the costs associated with the $\hat{\epsilon}$-quantile and ϵ-quantile, respectively. Each subfigure in Figure 7 contains two dashed lines: the left one represents the minimum threshold value υ^* among the 10 replications, and the right one represents the maximum threshold value υ^*. We observe that all the figures have similar cost distributions. Given a fixed $|K|$, as the value of ϵ increases, the costs associated with both

the $\hat{\epsilon}$-quantile and ϵ-quantile decrease. Additionally, when the sample size $|K|$ increases from 50 to 100, the distance between the two dashed lines decreases. This means that $|K| = 100$ leads to a more stable and closer match between the costs associated with the $\hat{\epsilon}$-quantile and ϵ-quantile. We therefore conclude that having a sample size of $|K| = 100$ is sufficient from the standpoint of solution stability in the out-of-sample performance.

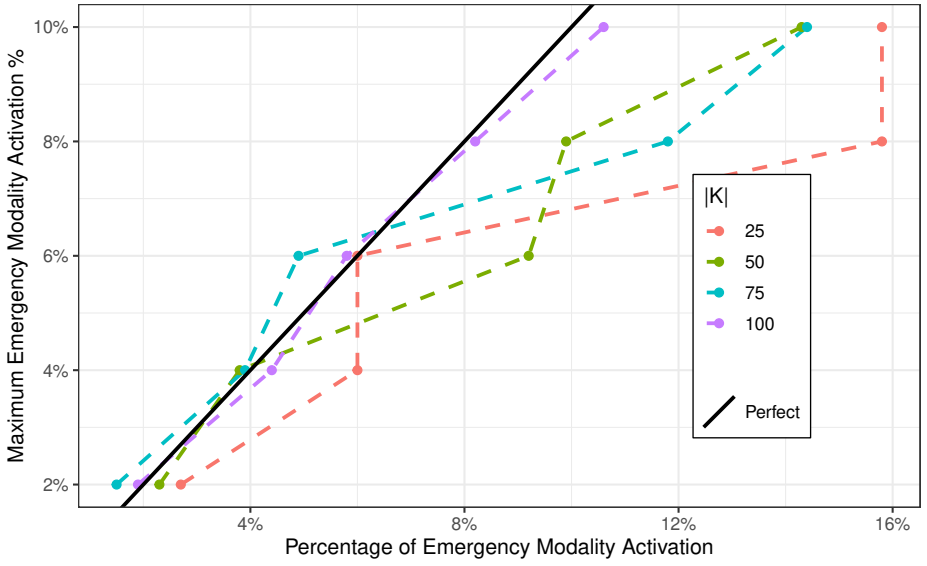

Figure 6: Solution Stability Reflected in the Out-of-sample Performance of the Threshold-based Policy.

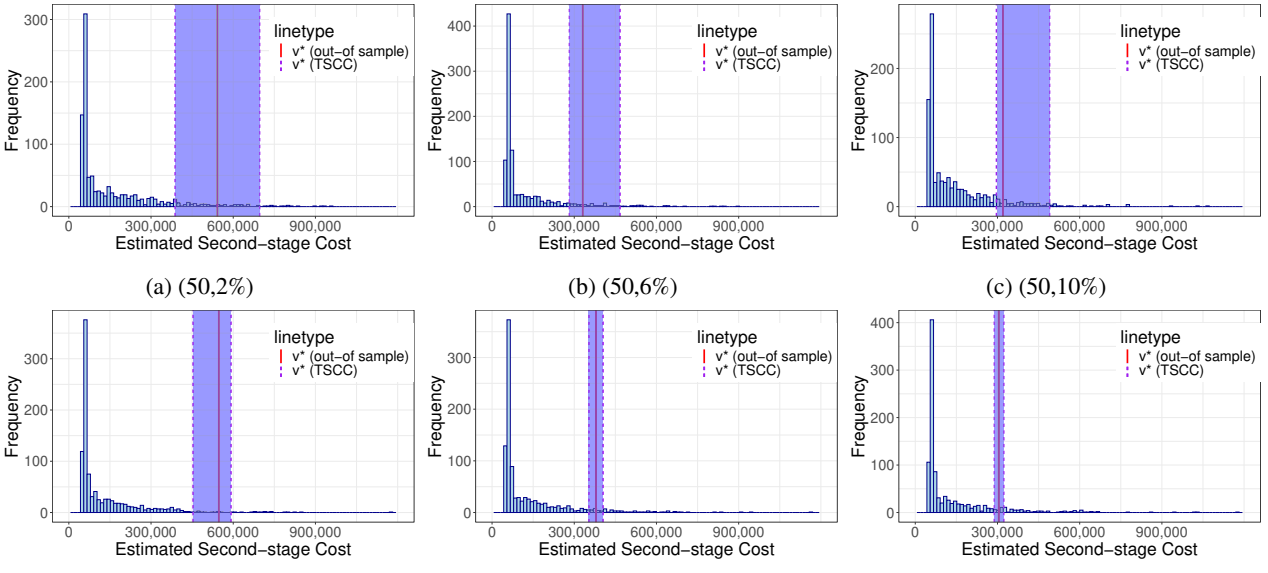

(a) (50,2%) (b) (50,6%) (c) (50,10%)

(d) (100,2%) (e) (100,6%) (f) (100,10%)

Figure 7: Cost Structure and Out-of-sample Stability Test of the Threshold-based Policy.

5.4.3. Comparison with Alternative Optimization Models

In this section, we present our experiment results for the proposed two-stage chance-constrained model (denoted as "TSCC") compared to the static (single-stage) chance-constrained model (denoted as "SS"), two-stage stochastic

programming model (denoted as "TS"), perfect-information model (denoted as "Perfect") and the wait-and-see model (denoted as "WS"). We test the performance of each model with the same set of scenarios sampled from the spatial regression model explained above. Specifically, the WS model makes no planning decisions and only makes acquisition and delivery decisions after collecting the actual housing demand (and therefore only operates in the second stage). The formulation of the WS model mirrors that of the TSCC, except that it sets the first-stage decision variables on acquisition and transportation to zero and activates the emergency modality in every scenario in the second stage. The TS model is the special case of the TSCC model with either no emergency modality allowed ($\epsilon = 0\%$) or the full flexibility of using the emergency modality ($\epsilon = 100\%$). Additionally, for the perfect-information model ("Perfect"), we solve a two-stage (deterministic) optimization model individually for each scenario, and then we compute the average across all scenarios (this is done for both the ordinary modality and the emergency modality). We note that for "Perfect", the first-stage decision has the (unrealistic) flexibility to adapt to each scenario due to its ability to foresee the demand realization in each scenario. While it is practically impossible to have the perfect information, this model provides a lower bound benchmark for all other models. Finally, the SS model is more involved, and we explain it in more details next.

The SS model considers the disaster housing preparation decisions only, aiming at satisfying the demand at a certain high percentage among all scenarios. It does not incorporate the post-disaster logistics costs and penalty costs that are involved in the second stage of TSCC. However, this does not imply that post-disaster logistics operations are ignored in the SS model. The constraints of delivery flow, staging area inventory capacity, and delivery flow limitations are crucial for deriving a feasible decision. Therefore, the goal in the SS model is to determine a decision that integrates both pre-disaster and post-disaster logistics, satisfying the demand at a certain high percentage among all scenarios. Thus, the formulation of SS is similar to that of the first-stage of TSCC. In addition, we incorporate the following constraints for SS.

$$\mu_{w,p,t+1} = \sum_{i\in I} x_{i,w,p,t-\Delta_{i,w}} \mathbb{1}(t-\Delta_{i,w} \geq 1) + \mu_{w,p,t}, \forall w \in W,\ t \in \mathcal{T}\backslash\{T_f\},\ p \in P \tag{16a}$$

$$\mu_{w,p,t+1} + \sum_{j\in J} f_{w,j,p,t+1} = \sum_{i\in I} x_{i,w,p,t-\Delta_{i,w}} \mathbb{1}(t-\Delta_{i,w} \geq 1) + \mu_{w,p,t},$$
$$\forall w \in W,\ t = T_f, T_f+1, \ldots, T-1,\ p \in P \tag{16b}$$

$$\sum_{p\in P} u_p \mu_{w,p,t} \leq U_w,\ \forall w \in W,\ t \in T \tag{16c}$$

$$\sum_{j\in J}\sum_{p\in P} \lambda_p f_{w,j,p,t} \leq \theta_w,\ \forall t \in \mathcal{T}_s, w \in W \tag{16d}$$

$$\sum_{w\in W} f_{w,j,n,t} = \sum_{h\in H} f^n_{j,h,t+\phi_{w,j}},\ \forall\, t \in \mathcal{T}_s,\ j \in J,\ n \in N \tag{16e}$$

$$d_{j,h,t+1} = d_{j,h,t} + \frac{1}{B_{n,h}} f^n_{j,h,t-\phi_{n,h}} \mathbb{1}(t-\phi_{n,h} \geq T_f+1) + \sum_{w\in W} f_{w,j,h,t-\Delta_{w,j}} \mathbb{1}(t-\Delta_{w,j} \geq T_f+1),$$
$$\forall j \in J,\ t \in \mathcal{T}_s\backslash\{T\},\ h \in H \tag{16f}$$

$$d_{j,h,T_d} \geq D^k_{j,h}(1-z_k),\ \forall j \in J,\ h \in H,\ k \in K \tag{16g}$$

$$f_{w,j,p,t} = 0,\ \text{if } t+\Delta_{w,j} \geq T,\ \forall w \in W, j \in J, p \in P, t \in T \tag{16h}$$

$$f^n_{j,h,t} = 0,\ \text{if } t+\phi_{n,j} \geq T,\ \forall j \in J, h \in H, t \in T \tag{16i}$$

Constraints (16a) and (16b) keep track of the number of each type of house at the staging area at each time period, and constraint (16c) incorporates the capacities of the staging areas. Every delivery for staging area w at each time t is bounded by its delivery capacity via constraints (16d). Constraint (16e) models the assignment of the AMHs to serve the purpose of the existing houses, and constraint (16f) represents the assignment of delivered houses to victims and captures the number of houses received at each demand node at each time t. Constraint (16g) ensures that the total number of received houses at each demand node by time T_d is more than the actual demand for each scenario k with $z_k = 0$.

To facilitate a fair comparison with TSCC, we compute the total cost of the solution obtained by incorporating planning decisions from the SS model into the TSCC model's first-stage solution. To be more specific, we plug in the

Model	ϵ	Total Cost	First-stage Cost	Second-stage Cost	Emergency Cost	Penalty Cost	Unused Cost	Unmet Cost	Deprivation Cost
TSCC	2%	853898	66.18%	33.82%	0.80%	19.02%	0.16%	16.23%	2.62%
	4%	843998	66.97%	33.03%	1.52%	17.58%	0.16%	14.88%	2.53%
	6%	834215	67.76%	32.24%	2.21%	16.16%	0.17%	13.56%	2.44%
	8%	824870	68.52%	31.48%	2.84%	14.76%	0.16%	12.56%	2.35%
	10%	817715	69.11%	30.89%	3.36%	13.64%	0.16%	11.22%	2.27%
SS	2%	1434060	90.79%	9.21%	0.01%	1.78%	1.03%	0.19%	0.56%
	4%	1427836	89.52%	10.48%	0.01%	2.06%	1.02%	0.36%	0.67%
	6%	1419250	89.94%	10.06%	0.10%	2.65%	1.03%	0.96%	0.66%
	8%	1416316	88.99%	11.01%	0.15%	2.71%	1.03%	1.03%	0.66%
	10%	1269116	87.54%	12.46%	0.29%	3.75%	0.89%	2.01%	0.85%
WS	-	637280	0.00%	100.00%	100.00%	0.00%	0.00%	0.00%	0.00%
TS	0%	864731	65.36%	34.64%	0.00%	20.58%	0.16%	17.72%	2.70%
	100%	627238	0.86%	99.14%	99.14%	0.00%	0.00%	0.00%	0.00%
Perfect(Ordinary)	-	781771	69.08%	30.92%	0.00%	30.92%	15.14%	12.44%	2.69%
Perfect(Emergency)	-	627044	1.75%	98.25%	98.25%	0.00%	0.00%	0.00%	0.00%

Table 3
Performance Comparison between models TSCC, SS, WS, TS, and Perfect.

solution to the SS model into the TSCC model as the first-stage solution. Subsequently, we solve the TSCC model with the same remaining constraints.

Table 3 shows the total expected cost, as well as the breakdowns of the first-stage cost and penalty costs under various choices of ϵ with $|K| = 50$. We note that all the values associated with costs are presented using thousand \$ as the unit in Table 3 and subsequent tables. Comparing TS with $\epsilon = 0\%$ to TSCC, TS with $\epsilon = 0\%$ has higher unmet penalty cost. Due to the absence of an emergency modality, there is no emergency acquisition to reduce unmet demand in extreme scenarios. Consequently, although the proportion of preparation costs in the total costs is nearly the same for both TSCC and TS with $\epsilon = 0\%$, TS with $\epsilon = 0\%$ incurs a higher unmet penalty cost, resulting in an overall higher penalty cost. On the other hand, comparing TS with $\epsilon = 100\%$ to TSCC, since the emergency modality is activated in all scenarios, only minimal preparation is required in the first stage, and the high demand in extreme scenarios can be fulfilled by emergency acquisition. Thus, TS with $\epsilon = 100\%$ has a significant emergency cost, low first-stage cost, and zero penalty cost. The cost structure of WS is similar to that of TS with $\epsilon = 100\%$. However, as a result of simply waiting (i.e., no preparation) in the first stage, WS misses the opportunity to have the minimal preparation that TS does, leading to higher overall cost than TS. Through comparing WS, TS and TSCC, it appears that higher activation percentages of emergency modality lead to lower overall costs, which may suggest that utilizing the TS model with $\epsilon = 100\%$ for planning is preferable. However, this overlooks the fact that the emergency modality is associated with significant additional resource allocation, and therefore, activating the emergency modality plan incurs significant extra cost. This activation cost is implicitly modeled in the TSCC model via the risk tolerance parameter ϵ, which provides an upper limit on the likelihood of emergency modality activation among all the scenarios. Additionally, we can observe the expected value of perfect information by comparing Perfect (Ordinary) and TS with $\epsilon = 0\%$ and comparing Perfect (Emergency) and TS with $\epsilon = 100\%$. We can see that with the emergency modality, due to the additional resources activated, the (expected) value of perfect information is not significant, and this is due to the minimal level of first-stage preparation operation needed. However, with the ordinary modality only, a significant amount of first-stage preparation operation becomes necessary in minimizing the overall cost, and the (expected) value of perfect information becomes significant.

Comparing SS to TSCC, we see that the decisions obtained from SS ignores various important factors such as the unmet penalty cost and the unused penalty cost. This results in a missed opportunity to optimize logistics effectively by balancing operational decisions and penalty cost in the second stage, leading to significantly higher first-stage costs for SS. Furthermore, in the SS model, the absence of emergency considerations in the planning phase leads to an inefficient utilization of the emergency modality plan. In comparison to the TSCC model, SS incurs a higher first-stage cost and a higher cost associated with the emergency modality plan. Unlike SS, TSCC makes acquisition and logistics decisions by considering the second-stage recourse decisions with two possible modalities, and incorporating unmet penalty, and unused penalty costs. Overall, we observe that TSCC leads to more effective logistics decisions.

Type	Trailer				MHU			
Model	SR	SRF	SVM	GNN	SR	SRF	SVM	GNN
MSE	0.0002	0.0063	0.0006	0.2405	0.0014	0.0028	0.0015	0.0024
RMSE	0.0387	0.2503	0.0770	0.1551	0.1194	0.1688	0.1234	0.1547

Table 4
The MSE/RMSE Comparison between Different Prediction Models.

Model	Total Cost	First-Stage Cost	Second-Stage Cost	Emergency Cost	Unused Cost	Unmet Cost	Deprivation Cost
Perfect	214067	173394	32944	0	0	0	0
GNN	687849	584671	103177	0	68784	0	0
SRF	632691	569421	63269	0	25307	0	0
SVM	444856	102316	342539	0	0	306950	13345
SR(Point)	605342	538754	605342	0	18160	0	0
SR	311749	268104	43644	0	3117	0	0

Table 5
Performance Comparison between Different Prediction Models with the Ordinary Modality.

Model	Total Cost	First-Stage Cost	Second-Stage Cost	Emergency Cost	Unused Cost	Unmet Cost	Deprivation Cost
Perfect	191075	0	191075	191075	0	0	0
GNN	206421	32712	173709	161281	0	0	0
SRF	194449	30572	163877	158119	0	0	0
SVM	192042	9562	182480	181077	0	0	0
SR(Point)	191083	126	190958	190952	0	0	0
SR	191075	0	191075	191075	0	0	0

Table 6
Performance Comparison between Different Prediction Models with the Emergency Modality.

5.5. Comparison with Alternative Prediction Models

In this section, we compare the proposed spatial regression model with alternative prediction models and investigate the impact of prediction accuracy on decision making in the context of the disaster housing assistance planning problem. First, we present the mean squared error (MSE) and root mean squared error (RMSE) metrics for different prediction models. Subsequently, we compare the operational decisions derived from these models following the predict-and-optimize framework.

We compare the spatial regression model used in our numerical experiments with alternative machine learning models, including spatial random forest regression, support vector machine regression, and graph neural networks. All models are implemented in R using the following packages: (i) Bivand, Millo, and Piras (2021); Bivand and Piras (2015); Bivand, Hauke, and Kossowski (2013a); Bivand, Pebesma, and Gómez-Rubio (2013b); Pebesma and Bivand (2023) for spatial regression models; (ii) Wright and Ziegler (2017); Benito (2021) for the spatial random forest model; (iii) Meyer, Dimitriadou, Hornik, Weingessel, and Leisch (2022) for support vector machine regression; and (iv) Falbel and Luraschi (2023) for the graph neural network model. All models are used default setting from these packages. For the graph neural network model, we have three layers. Each layer aggregates features from the neighboring nodes, applies a linear transformation to these aggregated features, and subsequently employs a ReLU activation function. The network starts with five input features, then expands to 32 features, then to 64 features, and finally aggregates to produce a single output.

Table 9 provides the prediction error results in terms of the mean squared error (MSE) and the root mean squared error (RMSE) for different prediction models. In this table, we use the following abbreviations for the different prediction models: (i) **SR** for spatial regression; (ii) **SRF** for spatial random forest regression; (iii) **SVM** for support vector machine; (iv) **GNN** for graph neural network. From the table, we can see that **SR** and **SVM** achieved the smallest prediction error in terms of the MSE and RMSE.

To understand the impact of these predictions on decision making, it is essential to examine the difference in the cost structure between decisions derived under perfect information and decisions derived from the predictive information provided by the prediction model. In the context of our problem, the decisions under perfect information can be derived by solving a two-stage (deterministic) optimization model with the exact housing demand information. For **SVM**, **SRF**, and **GNN**, we follow the predict-and-optimize framework by solving the two-stage (deterministic) model using the point prediction given by these prediction models, and then we evaluate the corresponding first-stage housing preparation decisions. For **SR**, we generate a set of demand realization scenarios (in our experiment we use sample size $|K| = 50$) by sampling the error term in the spatial regression model, solve a two-stage stochastic programming model (same as the TS model in Table 3) with these scenarios, and then evaluate the corresponding first-stage housing preparation decision with the exact realized housing demand information. Note that the numbers presented here are different from the ones shown in Table 3, which represent the expected costs with respect to the associated set of scenarios used in the TS model. To assess the solution quality of the housing preparation decisions associated with these prediction models, we evaluate them in the two-stage (deterministic) optimization model with the exact housing demand information, i.e., the same model where the perfect information solution is obtained from. For the sake of comparison, we consider a single modality here, either the ordinary or emergency modality, and Tables 5 and 6 show the cost structures of the solutions obtained under different prediction models with the ordinary modality and the emergency modality, respectively.

In Tables 5 and 6, **Perfect** represents the perfect-information model with the exact demand realization information. In addition to **SR**, **GNN**, **SRF** and **SVM** that we describe above, we also consider **SR(Point)**, in which the solution is derived solely from employing the point estimation from the spatial regression model using the deterministic two-stage optimization model instead of a two-stage stochastic program with a set of scenarios (as what is done in **SR**). From Table 5, where the ordinary modality is considered, we see that the solution employing **GNN** and **SRF** tends to exhibit overpreparation, consequently incurring higher penalty costs due to unused resources. This observation also implies an overestimation of housing demand by these two models. In contrast, the SVM-based model shows underpreparation, leading to increased penalty from unmet demands. Additionally, the solution employing **SR**, which exhibits comparable MSE and RMSE to **SVM**, has a cost structure closest to **Perfect**. However, for **SR(Point)**, which uses the same prediction model with **SR** but only employs only the point estimate, the cost structure resembles that of **SRF**, indicating overpreparation. Therefore, integrating the variability information (represented by the set of employed scenarios) into the optimization model helps alleviate the impact of the prediction error on decision making. On the other hand, based on the result in Table 6, where the emergency modality is considered, the prediction errors by different prediction models do not significantly impact the performance of the corresponding solution. This is due to the available resources that are activated from the emergency modality, which make the (first-stage) housing preparation decisions less crucial – as we can see from Table 6, the first-stage cost is insignificant in all options compared to the case when only the ordinary modality is used.

5.6. Sensitivity Analyses

In this section, we present the results from two types of sensitivity analyses. In Section 5.6.1, we perform the sensitivity analysis of the model with and without incorporating the AMHs. In Section 5.6.2, we perform the sensitivity analyses of various penalty cost parameters.

5.6.1. Incorporating Alternative Modular Housing Solutions

Table 7 shows the total expected cost with and without incorporating LiV, a specific type of AMH in our case study. We set $|K| = 50$ and use the abbreviation **Total Housing Prep.** in Table 7 to represent the percentage of the total number of houses prepared in the first stage with respect to the total expected housing demand.

In Table 7, we observe a notable decrease in the overall cost with the incorporation of LiV for both TSCC and SS. As the ϵ value increases from 2% to 10%, we see that TSCC and SS achieve a reduction of approximately 22% to 26% and 0.4% to 7%, respectively. We note that there is no cost reduction by incorporating AMH units in the case of WS (and we chose not to present the results in the table for this reason). This is because WS makes decisions only after the actual housing demand becomes realized, but the AMH solutions such as Liv, which involve higher costs in exchange for their flexibility to accommodate demand uncertainty, do not exhibit any advantage for WS when equipped with the exact demand realization information. Additionally, from observing the **Total Housing Prep**, it is noted that the inclusion of AMHs in both the TSCC and SS models does not significantly increase the number of house preparations, particularly in SS. Although there is a rise in the proportion of deprivation penalty costs within the overall cost due

Model	Modular	ϵ	Total Cost	First-stage Cost	Unused Cost	Unmet Cost	Deprivation Cost	Total Housing Prep
TSCC	With	2%	853898	66.18%	0.16%	16.23%	2.62%	28.12%
	W/o		1090230	71.43%	0.30%	17.60%	1.28%	29.45%
	With	4%	843998	66.97%	0.16%	14.88%	2.53%	28.07%
	W/o		1081252	71.72%	0.29%	16.94%	1.23%	29.90%
	With	6%	834215	67.76%	0.17%	13.56%	2.44%	27.98%
	W/o		1073499	72.67%	0.30%	15.25%	1.17%	29.90%
	With	8%	824870	68.52%	0.16%	12.26%	2.44%	29.53%
	W/o		1065326	72.73%	0.29%	14.61%	1.09%	29.88%
	With	10%	817715	69.11%	0.16%	11.22%	2.35%	27.97%
	W/o		1057858	71.03%	0.20%	16.06%	1.10%	26.23%
SS	With	2%	1434060	90.79%	1.03%	0.19%	0.56%	45.31%
	W/o		1584302	88.78%	1.53%	1.58%	0.76%	44.59%
	With	4%	1427836	89.52%	1.02%	0.36%	0.67%	44.40%
	W/o		1512016	89.17%	1.43%	1.15%	0.71%	43.48%
	With	6%	1419250	89.94%	1.03%	0.96%	0.66%	43.97%
	W/o		1445291	89.71%	1.52%	0.37%	0.71%	43.48%
	With	8%	1416316	88.99%	1.03%	1.03%	0.66%	43.48%
	W/o		1422631	89.90%	1.41%	0.21%	0.66%	42.12%
	With	10%	1269116	87.54%	0.89%	2.01%	0.85%	39.53%
	W/o		1293346	88.06%	1.29%	1.17%	0.83%	39.64%

Table 7
Cost Composition with and without Alternative Modular Housing Solutions (in Thousand $).

Parameter	Factor	Total Cost	First-Stage Cost	Second-Stage Cost	Unused Cost	Unmet Cost	Deprivation Cost	Unused Modular Houses	Unused Trailers	Unused MHUs	Unmet Demand Trailers	Unmet Demand MHUs
Deprivation Penalty	0.2	809177	564832	*244345*	1278	101059	*3999*	2.57%	0.00%	6.96%	*15.00%*	*0.00%*
	0.5	815132	564997	*250135*	1278	101059	*9789*	2.57%	0.00%	6.96%	*15.00%*	*0.00%*
	1	824870	565187	*259683*	1305	101090	*19368*	2.52%	0.00%	7.21%	*15.00%*	*0.00%*
	2	844180	565444	*278737*	1410	101260	*38401*	2.56%	0.00%	7.94%	*15.03%*	*0.00%*
	5	901654	565594	*336060*	1491	101575	*95520*	2.63%	0.00%	8.47%	*15.08%*	*0.00%*
Unmet Penalty	0.2	420176	*38955*	381221	0	*286599*	67739	0.00%	0.00%	0.00%	*86.18%*	*82.31%*
	0.5	641165	*366420*	274746	691	*131601*	18086	0.00%	0.00%	5.07%	*37.83%*	*0.14%*
	1	824870	*565187*	259683	1305	*101090*	19368	2.52%	0.00%	7.21%	*15.00%*	*0.00%*
	2	884840	*551492*	333347	2042	*182791*	18174	4.35%	0.00%	10.90%	*13.57%*	*0.00%*
	5	986115	*672262*	313853	4802	*172211*	12228	11.92%	0.03%	24.03%	*4.95%*	*0.06%*
Unused Penalty	0.2	832323	*574473*	257850	*2068*	99366	19595	*7.57%*	*0.00%*	*8.04%*	14.75%	0.00%
	0.5	834602	*573249*	261353	*1623*	100009	21516	*4.96%*	*0.00%*	*7.24%*	14.84%	0.00%
	1	824870	*565187*	259683	*1305*	101090	19368	*2.52%*	*0.00%*	*7.21%*	15.00%	0.00%
	2	836459	*573128*	263331	*1324*	102510	19641	*2.56%*	*0.00%*	*7.31%*	15.22%	0.00%
	5	835818	*568989*	266829	*1286*	101766	19657	*2.55%*	*0.00%*	*7.04%*	15.11%	0.00%

Table 8
Sensitivity Analyses on the Deprivation Penalty Factor and Unmet Demand Penalty Factor.

to the installation time requirement of the AMHs, for both models, the adoption of these more flexible AMHs not only reduces the proportion of preparation cost within the overall cost but also decreases the proportion of unused and unmet penalty costs. In sum, we observe from this set of sensitivity analyses the value of AMHs under the inherent uncertainty of housing demand due to their flexibility.

5.6.2. Sensitivity Analyses on Key Parameters

Table 8 presents the results concerning the impacts of various key parameters, including the deprivation penalty, unmet penalty, and unused penalty parameters. In this table, we use the following abbreviations for the column titles: (i) **Factor**: multiplier applied to the original parameter setting; (ii) **Unused AMHs/Trailers/MHUs**: the average percentage of AMHs/Trailers/MHUs left unused across all scenarios; (iii) **Unmet Trailers/MHUs**: the average percentage of unmet demand in Trailers/MHUs across all scenarios. The baseline setting for these parameters, which corresponds to a factor of 1, follows what is described in Section 5.3.

From Table 8, we observe the impacts of various penalty parameters and on the cost structure. For the deprivation penalty, increasing the deprivation penalty factor directly increases the second-stage cost. As the deprivation penalty increases, the logistics operational decisions are adjusted to expedite the arrival of the houses to the victims, aiming to minimize the deprivation costs. For the unmet penalty parameter, adjustments to the penalty factor directly influence the amount of unmet trailers and MHUs as well as the first-stage cost. Specifically, as the unmet penalty factor increases, a greater number of houses are prepared to avoid potential unmet penalty costs. It is noteworthy that with factor=0.2,

there is a considerable increase in unmet MHUs compared to the baseline setting, surging to 82.31%. This is because the unmet demand penalty in this setting falls below the acquisition price of a house, discouraging additional acquisitions of MHUs, that is, only the ones from the existing inventory at the permanent warehouses are utilized. For the unused penalty, due to current FEMA practices, we initially set the value in the baseline model to a relatively small level, resulting in insignificant difference in total cost. Despite its insignificance, changes of the unused penalty factor directly influence the increase or decrease of unused housing units: when the factor increases from 0.2 to 5, it results in a decrease from 7.57% to 2.55% and 8.04% to 7.04% for unused AMHs and MHUs, respectively.

We close this section by noting that the sensitivity analyses conducted here are particularly useful for addressing the disparities of community resilience against natural disasters in different regions, since individuals may exhibit different tolerances for housing demand shortages or deprivation. The TSCC model can generate the corresponding acquisition and logistical decisions to accommodate these differences by adjusting the penalty parameters. For example, when an anticipated housing shortage in a region is considered unacceptable, we may increase the unmet penalty parameter until the housing deficit reaches an acceptable threshold. Hence, the adjustments facilitates a balance between victims' priorities and the overall incurred costs, allowing the decision-maker to identify an optimal solution under different circumstances.

6. Conclusion

In this work, we have proposed a modeling and solution framework for the direct temporary disaster housing logistics planning problem under demand uncertainty. We have formulated the problem as a two-stage chance-constrained stochastic program with disaster housing demand scenarios generated in a data-driven fashion based on a spatial regression model that characterizes the correlation of disaster housing demand on a selected set of hazard quantification and socioeconomic factors. We have conducted an extensive numerical experiment with a case study for Hurricane Ian, based on which we have shown the advantage of the proposed model compared to some alternative approaches.

From a methodological perspective, we have identified two future directions that could further enhance this research. The first direction is to enhance the robustness of a model and hedge against the ambiguity of the demand distribution. In Section 5.4.2, the out-of-sample scenarios are generated from the same distribution as the in-sample scenarios, which corresponds to the error term in the employed spatial regression model. However, the out-of-sample test fails to account for the impact of the discrepancies between the training and test environments. A distributionally robust optimization (DRO) (Rahimian and Mehrotra, 2019) framework can be applied to address this issue, which is particularly valuable in making operational decisions where demand uncertainty could significantly impact decision-making. The second direction is to integrate the prediction model into an optimization framework. For example, following Sadana, Chenreddy, Delage, Forel, Frejinger, and Vidal (2024), there are two different paradigms for such integration: (i) a decision-rule based optimization approach, which applies a parameterized mapping as the decision rule and determining the parameter that optimizes the empirical performance based on available data; (ii) an integrated learning and optimization approach, which aims to identify a predictive model guiding contextual stochastic optimization problems toward optimal actions rather than precision in prediction alone. By integrating the prediction model into an optimization framework, we can potentially enhance the robustness and effectiveness of our model in handling demand uncertainty.

From a modeling perspective, we have identified two future research directions that expand the scope of logistics planning for direct temporary disaster housing. First, the proposed two-stage stochastic programming model can be extended to a multi-stage stochastic optimization model to capture additional information resolution during the disaster housing preparation and logistics operation, such as the uncertainty on funding availability. Second, while the short-term logistic plan equips us with the ability to address housing demand resulting from anticipated disaster displacement, transitioning to a more efficient planning strategy requires adopting a long-term perspective. Effective long-term disaster housing inventory planning can enhance the stability of our short-term logistical supply, thereby reducing both time and cost. However, unlike other consumed disaster relief resources, the aftermath of disaster housing must be address since it can only be provided for a maximum period of 18 months, governed by the Stafford Act (FEMA, 2019). Hence, in the planning of long-term disaster housing inventory, it is imperative to contemplate a broader spectrum of actions in comparison to other disaster relief resource planning. This includes considerations of housing for reimbursement, retrieval and acquisition, and presents an opportunity to explore alternative housing solutions that feature the transition from temporary to permanent solutions.

Acknowledgement. This work was partially supported by the National Science Foundation under grant agreement CMMI 2053660. Any opinions, findings, and conclusions or recommendations expressed in this paper are those of the authors and do not necessarily reflect the views of the National Science Foundation.

References

F. M. Deng, The global challenge of internal displacement, Wash. UJL & Pol'y 5 (2001) 141.

M. Hori, M. J. Schafer, Social costs of displacement in Louisiana after Hurricanes Katrina and Rita, Population and environment 31 (2010) 64–86.

FEMA, FEMA direct housing guide, https://www.fema.gov/sites/default/files/2020-07/Direct_Housing_Guide_Feb2020.pdf, 2020.

H. Katrina, Ineffective FEMA Oversight of Housing Maintenance Contracts in Mississippi Resulted in Millions of Dollars of Waste and Potential Fraud, Technical Report, GAO-08-106, November, 2007.

Laura Layden, With FEMA housing slow to arrive, most pass on the option in collier county, https://www.naplesnews.com/story/news/2022/12/22/fema-trailers-slow-to-arrive-in-collier-county-post-ian/69741960007/, 2022. Last accessed: October 24, 2023.

National Low Income Housing Coalition, FEMA continues to refuse to stand up disaster housing assistance program, https://nlihc.org/resource/fema-continues-refuse-stand-disaster-housing-assistance-program, 2018. Last accessed: October 24, 2023.

Pam Fessler, At least 100,000 homes were affected by Harvey. moving back in won't be easy, https://www.npr.org/2017/09/01/547598676/at-least-100-000-homes-were-affected-by-harvey-moving-back-in-wont-be-easy, 2017. Last accessed: October 24, 2023.

Patrick Adcroft, Children exposed to Hurricane Sandy while in womb show higher rates of depression, ADHD: study, https://tinyurl.com/36376abn, 2022. Last accessed: October 24, 2023.

FEMA, OpenFEMA dataset: Housing assistance program data - owners - v2, https://www.fema.gov/openfema-data-page/housing-assistance-program-data-owners-v2, 2023. Last accessed: October 24, 2023.

M. Erwin, FEMA purchased more manufactured housing units than it needed in Texas after Hurricane Harvey, Office of Inspector General OIG-20-15, https://www.oig.dhs.gov/sites/default/files/assets/2020-03/OIG-20-15-Feb20.pdf, 2020.

By Ken Serrano, Asbury Park (N.J.) Press, Report: Huge housing gap for N.J. Sandy victims, www.usatoday.com/story/news/nation/2012/12/07/nj-sandy-victims-housing-gap/1753555/, 2012. Last accessed: October 24, 2023.

X. Liu, S. Küçükyavuz, J. Luedtke, Decomposition algorithms for two-stage chance-constrained programs, Mathematical Programming 157 (2016) 219–243.

E. Hendriks, M. Basso, D. Sposini, L. van Ewijk, H. Jurkowska, Self-built housing as an alternative for post-disaster recovery, in: No-cost housing conference, ETH Zürich, 30th June-1st July 2016, 2017, pp. 1–6.

S. Patel, M. Hastak, A framework to construct post-disaster housing, International Journal of Disaster Resilience in the Built Environment 4 (2013) 95–114.

E. Wagemann, Need for adaptation: transformation of temporary houses, Disasters 41 (2017) 828–851.

D. Félix, J. M. Branco, A. O. Feio, Temporary housing after disasters: A state of the art survey, Habitat International 40 (2013) 136–141.

D. Félix, D. P. Monteiro, J. M. Branco, R. Bologna, A. O. Feio, The role of temporary accommodation buildings for post-disaster housing reconstruction, Journal of Housing and the Built Environment 30 (2015) 683–699.

D. Perrucci, H. Baroud, A review of temporary housing management modeling: Trends in design strategies, optimization models, and decision-making methods, Sustainability (2020).

O. El-Anwar, L. Chen, Automated community-based housing response: offering temporary housing solutions tailored to displaced populations needs, Journal of Computing in Civil Engineering 30 (2016) 04016019.

D. V. Perrucci, H. Baroud, Temporary housing operations: A simulation-based inventory management approach using the newsvendor model, International Journal of Disaster Risk Reduction 65 (2021) 102512.

M. Vanajakumari, S. Kumar, S. Gupta, An integrated logistic model for predictable disasters, Production and Operations Management 25 (2016) 791–811.

D. Alem, A. Clark, A. Moreno, Stochastic network models for logistics planning in disaster relief, European Journal of Operational Research 255 (2016) 187–206.

J. A. Paul, M. Zhang, Supply location and transportation planning for hurricanes: A two-stage stochastic programming framework, European Journal of Operational Research 274 (2019) 108–125.

H. Yang, D. Duque, D. P. Morton, Optimizing diesel fuel supply chain operations to mitigate power outages for hurricane relief, IISE Transactions 54 (2022) 936–949.

S. Duran, M. A. Gutierrez, P. Keskinocak, Pre-positioning of emergency items for CARE international, Interfaces 41 (2011) 223–237.

D. J. Morrice, P. Cronin, F. Tanrisever, J. C. Butler, Supporting hurricane inventory management decisions with consumer demand estimates, Journal of Operations Management 45 (2016) 86–100.

C. G. Rawls, M. A. Turnquist, Pre-positioning of emergency supplies for disaster response, Transportation research part B: Methodological 44 (2010) 521–534.

J. Salmerón, A. Apte, Stochastic optimization for natural disaster asset prepositioning, Production and operations management 19 (2010) 561–574.

E. Sanci, M. S. Daskin, An integer L-shaped algorithm for the integrated location and network restoration problem in disaster relief, Transportation Research Part B: Methodological 145 (2021) 152–184.

M. Pouraliakbari-Mamaghani, A. Saif, N. Kamal, Reliable design of a congested disaster relief network: A two-stage stochastic-robust optimization approach, Socio-Economic Planning Sciences 86 (2023) 101498.

T. C. Sütiçen, S. Batun, M. Çelik, Integrated reinforcement and repair of interdependent infrastructure networks under disaster-related uncertainties, European Journal of Operational Research 308 (2023) 369–384.

G. A. Velasquez, M. E. Mayorga, O. Y. Özaltın, Prepositioning disaster relief supplies using robust optimization, IISE Transactions 52 (2020) 1122–1140.

Y. Wang, Z. S. Dong, S. Hu, A stochastic prepositioning model for distribution of disaster supplies considering lateral transshipment, Socio-Economic Planning Sciences 74 (2021) 100930.

S. F. Pernett, J. Amaya, J. Arellana, V. Cantillo, Questioning the implication of the utility-maximization assumption for the estimation of deprivation cost functions after disasters, International Journal of Production Economics 247 (2022) 108435.

A. Moreno, D. Alem, D. Ferreira, A. Clark, An effective two-stage stochastic multi-trip location-transportation model with social concerns in relief supply chains, European Journal of Operational Research 269 (2018) 1050–1071.

N. Pérez-Rodríguez, J. Holguín-Veras, Inventory-allocation distribution models for postdisaster humanitarian logistics with explicit consideration of deprivation costs, Transportation Science 50 (2016) 1261–1285.

D. Rivera-Royero, G. Galindo, R. Yie-Pinedo, A dynamic model for disaster response considering prioritized demand points, Socio-economic planning sciences 55 (2016) 59–75.

J. Holguín-Veras, N. Pérez, M. Jaller, L. N. Van Wassenhove, F. Aros-Vera, On the appropriate objective function for post-disaster humanitarian logistics models, Journal of Operations Management 31 (2013) 262–280.

J. Holguín-Veras, J. Amaya-Leal, V. Cantillo, L. N. Van Wassenhove, F. Aros-Vera, M. Jaller, Econometric estimation of deprivation cost functions: A contingent valuation experiment, Journal of Operations Management 45 (2016) 44–56.

M. Siddig, Y. Song, Multi-stage stochastic programming methods for adaptive disaster relief logistics planning, arXiv preprint arXiv:2201.10678 (2022).

J. Luedtke, A branch-and-cut decomposition algorithm for solving chance-constrained mathematical programs with finite support, Mathematical Programming 146 (2014) 219–244.

B. Zeng, Y. An, L. Kuznia, Chance constrained mixed integer program: Bilinear and linear formulations, and benders decomposition, arXiv preprint arXiv:1403.7875 (2014).

M. Davlasheridze, Q. Miao, Natural disasters, public housing, and the role of disaster aid, Journal of Regional Science 61 (2021) 1113–1135.

G. A. Kopp, S. H. Li, H. Hong, Analysis of the duration of high winds during landfalling hurricanes, Frontiers in Built Environment 7 (2021) 632069.

U.S. Census Bureau., H1 occupancy status, https://data.census.gov/, 2022. Last accessed: October 24, 2023.

National Oceanic and Atmospheric Administration., Best track data (hurdat2), https://www.nhc.noaa.gov/data/#hurdat, 2022. Last accessed: October 24, 2023.

The United States Geological Survey., USGS flood event viewer: providing hurricane and flood response data., https://stn.wim.usgs.gov/fev/, 2022. Last accessed: October 24, 2023.

The Centers for Disease Control and Prevention., CDC/ATSDR SVI data and documentation download., https://www.atsdr.cdc.gov/placeandhealth/svi/index.html, 2020. Last accessed: October 24, 2023.

P. A. Moran, Notes on continuous stochastic phenomena, Biometrika 37 (1950) 17–23.

L. Anselin, A. K. Bera, Introduction to spatial econometrics, Handbook of applied economic statistics 237 (1998).

Kimberly Kuizon, Sarasota County residents struggle without FEMA assistance one year after Hurricane Ian, https://tinyurl.com/43ppe8tw, 2023. Last accessed: October 24, 2023.

John Squerciati, P.E, Disaster recovery alternative housing study findings report, https://www.recovery.texas.gov/files/resources/planning/alternative-housing-study-findings-report.pdf, 2020. Last accessed: October 24, 2023.

Marissa Gluck., Liv-Connected's design-forward units are helping redefine modular housing., https://metropolismag.com/profiles/liv-connecteds-design-forward-units-are-helping-redefine-modular-housing/, 2023. Last accessed: October 24, 2023.

Texas General Land Office by Hagerty Consulting, Inc., Disaster recovery alternative housing study findings report, https://recovery.texas.gov/files/resources/planning/alternative-housing-study-findings-report.pdf, 2020. Last accessed: May 24, 2024.

Roy Diez., How long does it take to build a manufactured home?, https://www.newhomesource.com/learn/how-long-build-manufactured-home/#:~:text=One%20of%20the%20biggest%20advantages,an%20order%20with%20their%20builder., 2023. Last accessed: Febuary 26, 2024.

FEMA, Advance contracts of goods and services, https://www.fema.gov/businesses-organizations/doing-business/advanced-contracts, 2023.

FEMA, The latest statistics on FEMA's mobile home program - more than 2,500 households leave temporary FEMA units, return home, 2018. URL: https://tinyurl.com/35c4wt5b, last accessed: October 24, 2023.

Clemson University, About the palmetto cluster, https://docs.rcd.clemson.edu/palmetto/about/, 2024. Last accessed: Febuary 26, 2024.

R. Bivand, G. Millo, G. Piras, A review of software for spatial econometrics in R, Mathematics 9 (2021).

R. Bivand, G. Piras, Comparing implementations of estimation methods for spatial econometrics, Journal of Statistical Software 63 (2015) 1–36.

R. Bivand, J. Hauke, T. Kossowski, Computing the jacobian in gaussian spatial autoregressive models: An illustrated comparison of available methods, Geographical Analysis 45 (2013a) 150–179.

R. S. Bivand, E. Pebesma, V. Gómez-Rubio, Applied spatial data analysis with R, Second edition, Springer, NY, 2013b. URL: https://asdar-book.org/.

E. Pebesma, R. S. Bivand, Spatial Data Science With Applications in R, Chapman & Hall, 2023. URL: https://r-spatial.org/book/.

M. N. Wright, A. Ziegler, ranger: A fast implementation of random forests for high dimensional data in C++ and R, Journal of Statistical Software 77 (2017) 1–17.

B. M. Benito, spatialRF: Easy Spatial Regression with Random Forest, 2021. URL: https://blasbenito.github.io/spatialRF/. doi:10.5281/zenodo.4745208, r package version 1.1.3.

D. Meyer, E. Dimitriadou, K. Hornik, A. Weingessel, F. Leisch, e1071: Misc Functions of the Department of Statistics, Probability Theory Group (Formerly: E1071), TU Wien, 2022. URL: https://CRAN.R-project.org/package=e1071, r package version 1.7-12.

D. Falbel, J. Luraschi, torch: Tensors and Neural Networks with 'GPU' Acceleration, 2023. URL: https://CRAN.R-project.org/package=torch, r package version 0.12.0.

H. Rahimian, S. Mehrotra, Distributionally robust optimization: A review, arXiv preprint arXiv:1908.05659 (2019).

U. Sadana, A. Chenreddy, E. Delage, A. Forel, E. Frejinger, T. Vidal, A survey of contextual optimization methods for decision-making under uncertainty, European Journal of Operational Research (2024).

FEMA, Stafford Act, as amended, and related authorities, https://www.fema.gov/press-release/20230728/fema-staging-area-springs-life-housing-mission-draws-close-another-gains, 2019.

B. E. Flanagan, E. W. Gregory, E. J. Hallisey, J. L. Heitgerd, B. Lewis, A social vulnerability index for disaster management, Journal of homeland security and emergency management 8 (2011) 000010220215477355179 2.

A. Detailed solution approach

In this section, we describe the detailed branch-and-cut decomposition algorithm for solving the proposed two-stage chance-constrained stochastic program in Algorithm 1. Within Algorithm 1, we use functions BigM() and Specut() to represent the functions that generate big-M cuts (7) and special cuts (9), respectively. We also provide details on how to properly choose valid big-M parameters to use in the big-M cuts (7). Note that the relatively complete recourse property holds in our model, thus there is no need to discuss feasibility cuts.

Algorithm 1 Decomposition algorithm for TSCC

$t \leftarrow 0, \text{OPEN} \leftarrow \{0\}, \text{UB} \leftarrow \infty, \text{LB} \leftarrow -\infty$;
while OPEN $\neq 0$ **do**
  Pick $l \in \text{OPEN}, \text{OPEN} \leftarrow \text{OPEN}\backslash\{l\}$;
  while CUTFOUND $\neq$ TRUE & LB $\leq$ UB **do**
    $(\hat{x}, \hat{s}, \hat{\mu}, \hat{v}, \hat{z}, \hat{\theta}) \leftarrow$ Solve model (4);
    $LB \leftarrow M(K_0(l), K_1(l))$;
    for $k \in K$ **do**
      if $\hat{z}_k = 0$, $\pi^0_k \leftarrow$ Solve $f(\hat{x}, \hat{\mu}, k)$;
      if $\hat{z}_k = 1$, $\bar{\pi}^1_k \leftarrow$ Solve $\bar{f}(\hat{x}, \hat{s}, \hat{\mu}, \hat{v}, k)$;
    end for
    if $\frac{1}{|K|}\sum_{k\in K}\left((1-\hat{z}_k)f(\hat{x}, \hat{\mu}, k) + \hat{z}_k\bar{f}(\hat{x}, \hat{s}, \hat{\mu}, \hat{v}, k)\right) \geq \hat{\theta}$ **then**
      if $\hat{z}_k = 0$, $\bar{\pi}^0_k \leftarrow$ Solve $\bar{f}(\hat{x}, \hat{s}, \hat{\mu}, \hat{v}, k)$;
      if $\hat{z}_k = 1$, $\pi^1_k \leftarrow$ Solve $f(\hat{x}, \hat{\mu}, k)$;
      $L \leftarrow Specut(\bar{\pi}^0_k, \pi^1_k, \pi^0_k, \bar{\pi}^1_k), BigM(\pi^0_k, \bar{\pi}^1_k)$
    else
      CUTFOUND $\neq$ TRUE
      UB $\leftarrow$ LB
    end if
  end while
  if LB $\leq$ UB **then**
    Choose $k \in K$ *s.t.* $\hat{z}_k \in (0, 1)$
    $K_0(t+1) \leftarrow K_0(l) \cup \{k\}, K_1(t+1) \leftarrow K_1(l)$;
    $K_0(t+2) \leftarrow K_0(l) \cup \{k\}, K_1(t+2) \leftarrow K_1(l) \cup \{k\}$;
    $t \leftarrow t+2$;
    OPEN $\leftarrow$ OPEN $\cup\{t+1, t+2\}$
  end if
end while

We consider the following to derive a sufficiently large big-M value:

(1) By duality, $\pi^{(1d)}_{k,w,t}$ and $\bar{\pi}^{(2i)}_{k,i,t}$ are always nonpositive.

(2) Based on constraint (3g),
$\sum_{w\in W}\sum_{p\in P}\mu_{w,p,T_f}\pi^{(1b)}_{k,w,p} \leq \sum_{w\in W}\sum_{p\in P}\frac{U_w}{U_p}\pi^{(1b)}_{k,w,p}$.

	Variable	Type	Unit
Regressands	**Trailer Assistance Rate**	Numerical	Percentage
	MHU Assistance Rate		
Predictors	**High-water Mark**		ft
	Duration of Sustained Wind Speed		Day
	Distance to Landfall Location		Mile
	SVI (Social Vulnerability Index)		-
	Population		Person

Table 9
Description of Regressands and Predictors Used in the Spatial Regression Models.

(3) Based on constraint (3e),
$\sum_{w\in W}\sum_{p\in P}\sum_{t\in\mathcal{T}_s}(\sum_{i\in I} x_{i,w,p,t-\Delta_{i,w}}\mathbb{1}(t-\Delta_{w,j}\geq 1))\pi^{(1c)}_{k,w,t,p}$
$\leq \sum_{w\in W}\sum_{p\in P}\sum_{t\in\mathcal{T}_s}(\sum_{i\in I}\theta_i)\pi^{(1c)}_{k,w,t,p}$.

(4) Based on constraint (3c) and constraint (3j),
$\sum_{i\in I}\sum_{p\in P} v^k_{i,p,T_f}\bar{\pi}^{(2c)}_{k,i,p} \leq \sum_{i\in I}\sum_{p\in P}(E_i+V_{i,p})\bar{\pi}^{(2c)}_{k,i,p}$.

(5) Based on constraint (3i) and constraint (3j),
$\sum_{t\in\mathcal{T}_s}\sum_{p\in P}\sum_{i\in I}(s_{i,p,t-\tau_{i,p}}\mathbb{1}(t-\tau_{i,p}\geq 1)-\sum_{w\in W} x_{i,w,p,t+1})\bar{\pi}^{(2d)}_{k,i,t,p}$
$\leq \sum_{t\in\mathcal{T}_s}\sum_{p\in P}\sum_{i\in I}\sum_{w\in W} E_w\bar{\pi}^{(2d)}_{k,i,t,p}$.

According to the above consideration, the big-M values can be set as follows:

$$M_k = \sum_{w\in W}\sum_{p\in P}\frac{U_w}{U_p}\pi^{(1b)}_{k,w,p} + \sum_{w\in W}\sum_{p\in P}\sum_{t\in\mathcal{T}_s}\sum_{i\in I}\theta_i\pi^{(1c)}_{k,w,t,p} + \sum_{t\in\mathcal{T}_s}\sum_{j\in J}\sum_{g\in G} D^k_{j,g}\pi^{(1g)}_{k,j,g} \tag{17a}$$

$$\bar{M}_k = \sum_{w\in W}\sum_{p\in P}\frac{U_w}{U_p}\bar{\pi}^{(1b)}_{k,w,p} + \sum_{w\in W}\sum_{p\in P}\sum_{t\in\mathcal{T}_s}\sum_{i\in I}\theta_i\bar{\pi}^{(1c)}_{k,w,t,p} + \sum_{i\in I}\sum_{p\in P}(E_i+V_{i,p})\bar{\pi}^{(2c)}_{k,i,p}$$
$$+ \sum_{t\in\mathcal{T}_s}\sum_{p\in P}\sum_{i\in I}\sum_{w\in W} E_w\bar{\pi}^{(2d)}_{k,i,t,p} \tag{17b}$$

B. Data Description

Table 9 describes the regressands and predictors used in the spatial regression models, including their units and types. The SVI value is in the range between 0 and 1, which is derived from 15 different selected variables (Flanagan, Gregory, Hallisey, Heitgerd, and Lewis, 2011). Figure 9 presents the Spearman's correlation between regressands and predictors from the used dataset.

C. Sensitivity Analysis for the Initial Inventory Level

Based on the information from FEMA (2018), before housing units are deployed to fulfill the disaster housing needs, FEMA performs cleaning and quality inspections to these units. Therefore, the initial inventory level may fluctuate and it is important to understand how different initial inventory level may affect decision making and the associated cost structure. Table 10 presents the results for different initial inventory levels. From the table, it is evident that the first-stage cost and unmet cost decrease with increasing initial inventory: with more initial available inventory, it is expected that less housing preparation is made, and a larger number of houses could potentially be used for demand fulfillment, leading to a reduced unmet penalty cost as well.

D. Additional Illustrations

In this section, we provide some additional illustrations on the proposed optimization models and the problem data.

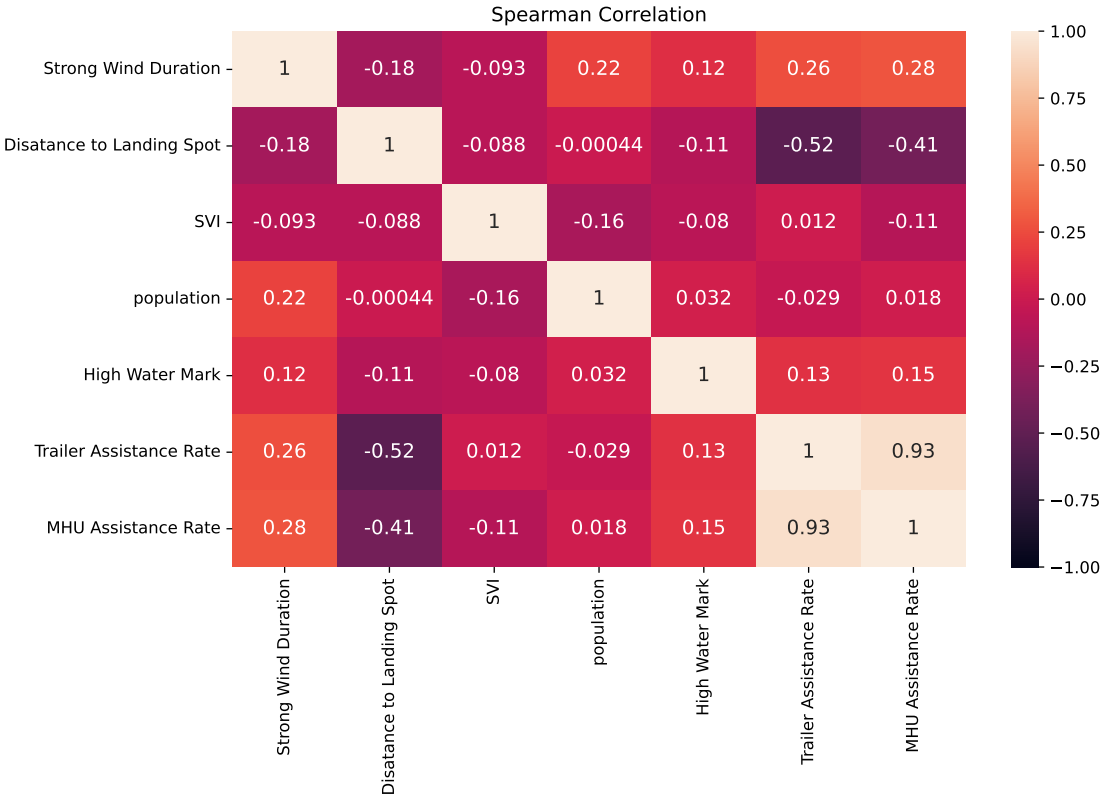

Figure 8: Spearman's Correlation between Factors and Predictors.

Initial Level	Total Cost	First-Stage Cost	Second-Stage Cost	Emergency Cost	Unused Cost	Unmet Cost	Deprivation Cost
120	837894	569767	268127	24299	1256	107501	20193
300	833597	576182	257415	23090	1667	100198	20152
600	820881	574431	257414	22757	1917	98531	19838
1200	804544	550927	253617	23091	1600	95701	19246
3000	733877	492142	241735	22729	1539	86630	17863

Table 10
Performance Comparison under Different Initial Inventory Level.

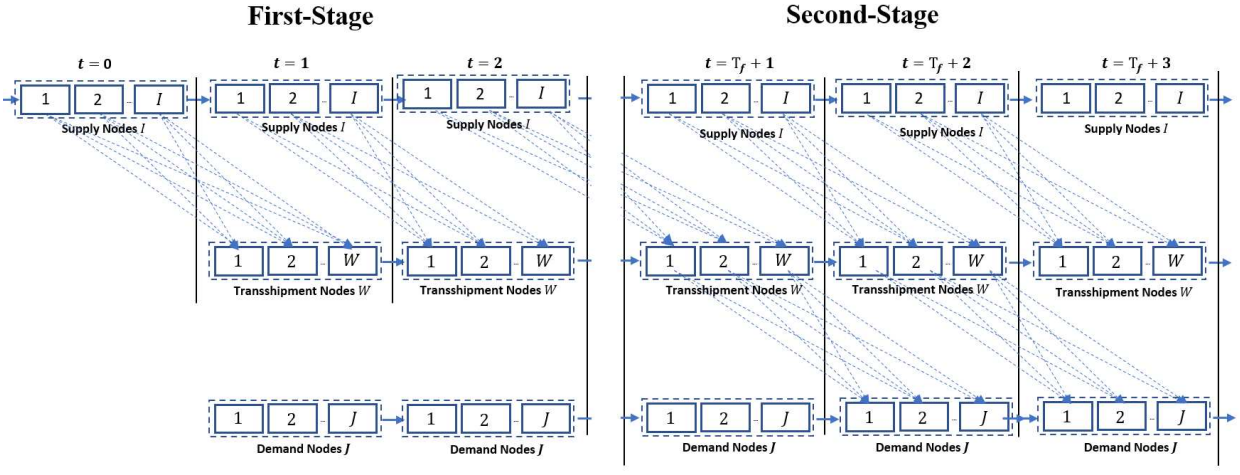

Figure 9: An illustration of the logistics flow in the proposed disaster housing logistics planning model (assuming $\Delta_{i,w} = 1$ and $\Delta_{w,j} = 1$ for all i, j, w).

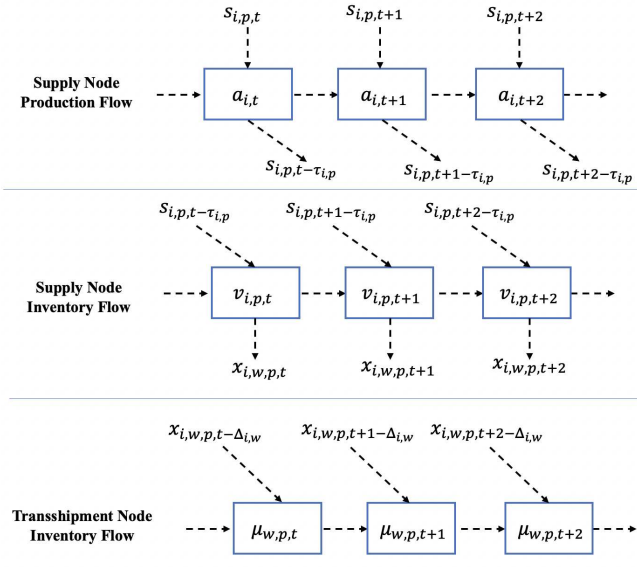

(a) First-stage Constraint Flows.

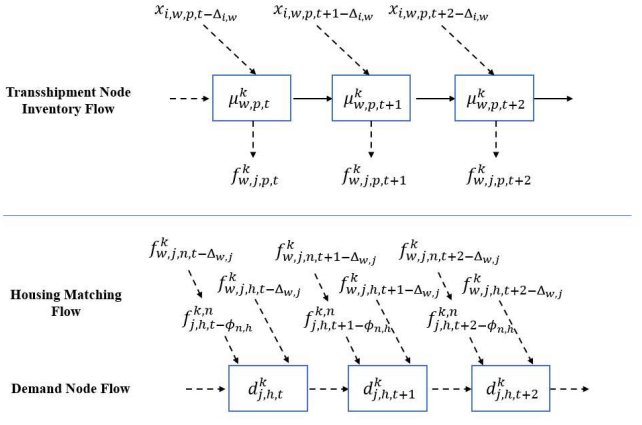

(b) Ordinary Modality Constraint Flows.

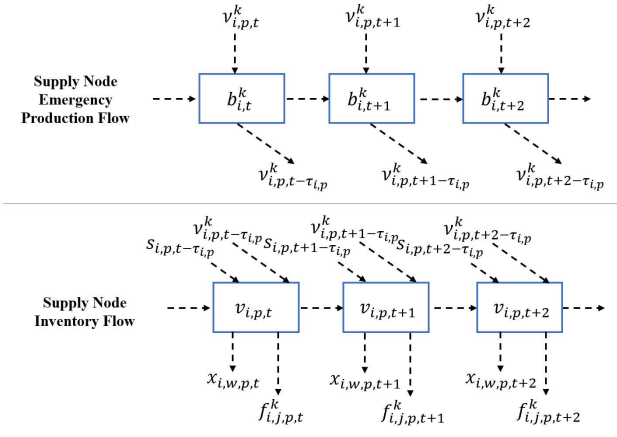

(c) Emergency Modality Constraint Flows.

Figure 10: Illustration of flow balance constraints in the proposed model.